

Graphene-based hybrid materials: synthetic approaches and properties

Kasinath Ojha¹, Oruganti Anjaneyulu¹ and Ashok K. Ganguli^{1,2,*}

¹Department of Chemistry, Indian Institute of Technology Delhi, Hauz Khas, New Delhi 110 016, India

²Institute of Nano Science and Technology, Phase-10, Sector- 64, Mohali 160 062, India

Carbon has a unique chemistry reflected in its wide presence in the inorganic and organic world – benzene, diamond, graphite, fullerene, carbon nanotubes and now graphene – carbon seems to be at the centre of action in the playground of scientific research. In this review, synthesis and unique properties of graphene and graphene-based composites have been discussed with particular emphasis on the environmentally benign (green) synthetic methods and their wide applications, especially in energy conversion, energy storage, electronics, biomedical and biosensing applications.

Keywords: Biosensing, gene delivery, graphene synthesis, Li-ion batteries, supercapacitors, water desalination.

Introduction

GRAPHENE, also called as ‘super carbon’¹, is one-atom thick two-dimensional sheet of carbon atoms fashioned in a honeycomb lattice and is considered as the future revolutionary material. An exponential growth after 2004 in graphene-related research is reflected in the number of publications (ISI *Web of Knowledge*)². Graphene having unique electronic properties like the absence of charge localization, half-integer quantum Hall effect, ultrahigh mobility in combination with outstanding mechanical properties compared to other carbon materials, has attracted enormous interest. The electronic properties of graphene are derived mainly from the π -electrons, which make it an ideal 2D system where the π -states form the valence band and the π^* states form the conduction band. In the band structure these two bands overlap at six points in k -space, which are called as Dirac points (zero band gap)³. The conduction electrons in graphene can travel near the speed of light and have zero effective mass and are also called Dirac fermions. Graphene is hence known as a Dirac solid. The other remarkable electrical and optical properties are its ballistic transport over $\sim 0.4 \mu\text{m}$ length, high carrier mobility at room temperature⁴ ($15,000 \text{ cm}^2 \text{ V}^{-1} \text{ s}^{-1}$), thermal conductivity¹ of $> 5000 \text{ W}/(\text{mK})$, wideband absorption (from visible to

near-infrared (NIR) regions) as well as good visual transparency⁵, quantum Hall effect at room temperature and single-molecule field-effect sensitivity. Graphene having very large surface area⁶ (theoretical surface area $\sim 2600 \text{ m}^2/\text{g}$) is effective for sensors, where all the carbon atoms can take part in the sensing and interaction with foreign molecules/species. Graphene can be considered for potential applications in both emerging and conventional fields like field-effect transistors^{7,8}, electrochemical devices⁹, electromechanical resonators, polymer nanocomposites¹⁰, batteries, ultracapacitors¹¹, biosensors¹² and light-emitting devices. Graphene-based flexible conducting electrodes are important for flexible electronic devices¹³. They have been applied for organic light-emitting diodes (OLED), capacitive sensors in touch-screen displays and for organic photovoltaic (OPV) devices. Graphene and graphene-based hybrids can be considered as potential candidates for replacing Si-based technologies due to their extraordinary properties. Outstanding carrier mobility, good transconductance of graphene devices, ultimate thinness (atomic level) and stability of the material are the main attractions of graphene. Graphene can be a revolutionary material for living beings as it is less toxic¹⁴, which can be manipulated chemically and, more importantly, it is biodegradable¹⁵. The toxicity of different forms and hybrids of graphene has been well documented¹⁴.

Graphene has been synthesized by different methods, including wet chemical and solid-state methods, chemical vapour deposition (CVD), metal-organic chemical vapour deposition (MOCVD) and mechanical exfoliation. Novoselov *et al.*⁴ reported a simple mechanical exfoliation technique using Scotch Tape to obtain supported single-layer graphene from graphite. The most followed gram-scale wet chemical synthesis of graphene from graphite powder via oxidation and reduction followed by exfoliation is known as Hummers method¹⁶. There are reports of graphene synthesis by thermal decomposition of silicon carbide (SiC) (solid-state method) and the generation of graphene layers on transition metals (CVD method). Lateral size, layer thickness homogeneity and purity are important for the high-end applications of graphene in electronics and devices¹⁷. In most electronic devices, indium tin oxide (ITO) has been used due to its low resistance ($10\text{--}30 \Omega \text{ sq}^{-1}$) and high optical transmittance

*For correspondence. (e-mail: ashok@chemistry.iitd.ac.in)

(>90% at 550 nm)¹⁸. Graphene can be a good choice and possible replacement of ITO¹⁹ as an electrode material as it is thermally and chemically stable, highly conductive, flexible and transparent.

In this article we discuss synthesis of graphene and its hybrid materials for their potential applications in different fields. We focus on the design of graphene-based hybrid materials, which is an important application of nanotechnology. Here we emphasize the relatively greener methods for synthesizing graphene-based materials. We also discuss recent developments in biological applications of graphene-based hybrids along with electronic, energy and environmental applications.

Synthesis

Properties and applications of any material are intimately related to its size, shape and morphology. Hence a materials chemist needs to have a basket of synthesis techniques to control size, shape and morphology of a material. Keeping commercial applications in mind, researchers need to develop synthetic routes which can give high-yield of graphene with good control over morphology. Graphite oxide chemistry is quite old and was first studied by Brodie^{20,21} in 1859. After this, several others like Staudenmaier, Hofmann and Frenzel, Hamdi and Hummers reported synthesis of graphite oxide from graphite under strong oxidizing agents in the presence of oxidants, with slight modifications in reaction conditions¹⁶.

Even though graphite and graphite oxide have a long history, monolayer graphene films were first discovered by Novoselov *et al.*²² in 2004 by the mechanical exfoliation of highly oriented pyrolytic graphite (HOPG). There is a burgeoning interest in graphene chemistry, which is evident from a special issue devoted to graphene (*Acc. Chem. Res.*, 2013, **46**, 1–190) and several reviews on graphene, graphene oxide and their derivatives^{23–42}. In the literature there are various methods reported on synthesis of graphene sheets and their derivatives, which include mechanical cleavage of graphite, unzipping carbon nanotubes⁴³, chemical exfoliation of graphite, solvothermal synthesis, epitaxial growth on SiC surfaces and metal surfaces, CVD of hydrocarbons on metal surfaces, bottom-up organic synthesis, electric arc discharge method, sonochemical approach, reduction of graphene oxide (GO) obtained from graphite oxide by chemical reducing agents, and aqueous and environment-friendly greener reduction methods. We discuss some of the popular methods of synthesis below.

Mechanical exfoliation or Scotch Tape method

The first method for the synthesis of monolayer graphene films was by micromechanical cleavage (Scotch Tape method) of highly oriented pyrolytic graphite (HOPG)²².

With slight modification, crystals of high structural and electronic quality of millimetre length graphene were obtained⁴⁴. These large samples can be used to fabricate high-speed ambipolar field-effect transistors⁴⁵ and also as sensors to detect individual gas molecules⁴⁶. It is a laborious, time-consuming, delicate approach and limited amount of graphene is produced; hence bulk production of graphene is difficult by mechanical exfoliation.

Chemical reduction of exfoliated graphite oxide

The most common method employed for the large-scale synthesis of graphene is by chemical exfoliation of graphite oxide. Graphite oxide can be produced by several methods like treating graphite with strong oxidizers such as sulphuric acid, nitric acid, potassium chlorate and potassium permanganate^{47–50}. Oxidation results in the introduction of oxygen-rich functional groups like carboxyl, epoxide and hydroxyl groups onto the graphene basal plane and edges. The graphite oxide produced still possesses the layered structure, but is lighter in colour than graphite due to loss of conjugation during oxidation as the change in hybridization of carbon atoms occurs from planar sp² to tetrahedral sp³. This also results in decrease in inter-layer interactions, which in turn increase the d-spacing as well as make it an electrical insulator^{48,51–53}. The oxygen functionalities alter the van der Waals interactions among the layers of graphite oxide and make it hydrophilic, thus facilitating their hydration and exfoliation in aqueous media. Due to this, graphite oxide forms stable colloidal dispersion in aqueous media as thin graphite oxide sheets^{54–57}. Liu and Gong⁵⁸ reported the reduction of polyaniline-intercalated graphite oxide in aqueous hydrazine hydrate (50% w/v). Ruoff and co-workers⁵¹ while preparing stable aqueous dispersions of graphitic nanoplatelets in the presence of poly(sodium 4-styrenesulfonate), also used hydrazine hydrate for the reduction of graphite oxide nanoplatelets prepared by exfoliation of the graphite oxide (Figure 1a). As the reduction proceeds, change in colour from brown to black was observed⁵¹. There are several other reports on reduction of graphite oxide by hydrazine hydrate^{48,59–65}. Stankovich *et al.*⁶ reported the utility of dimethylhydrazine as reducing agent for the reduction of graphene–polymer composite, viz. exfoliated phenylisocyanate-treated graphite oxide sheets with polystyrene⁶.

Sodium borohydride (NaBH₄) is one of the well-explored strong reducing agents. Cassagneau and Fendler *et al.*⁶⁶ reported the utility of NaBH₄ for the reduction of silver ions in aqueous dispersions of exfoliated graphite oxide nanosheets. Ajayan and co-workers⁶⁷ developed a novel strategy to explain the reduction mechanism of graphite oxide using NaBH₄ and treatment with sulphuric acid followed by thermal annealing (Figure 1b). This method is particularly effective in the restoration of the

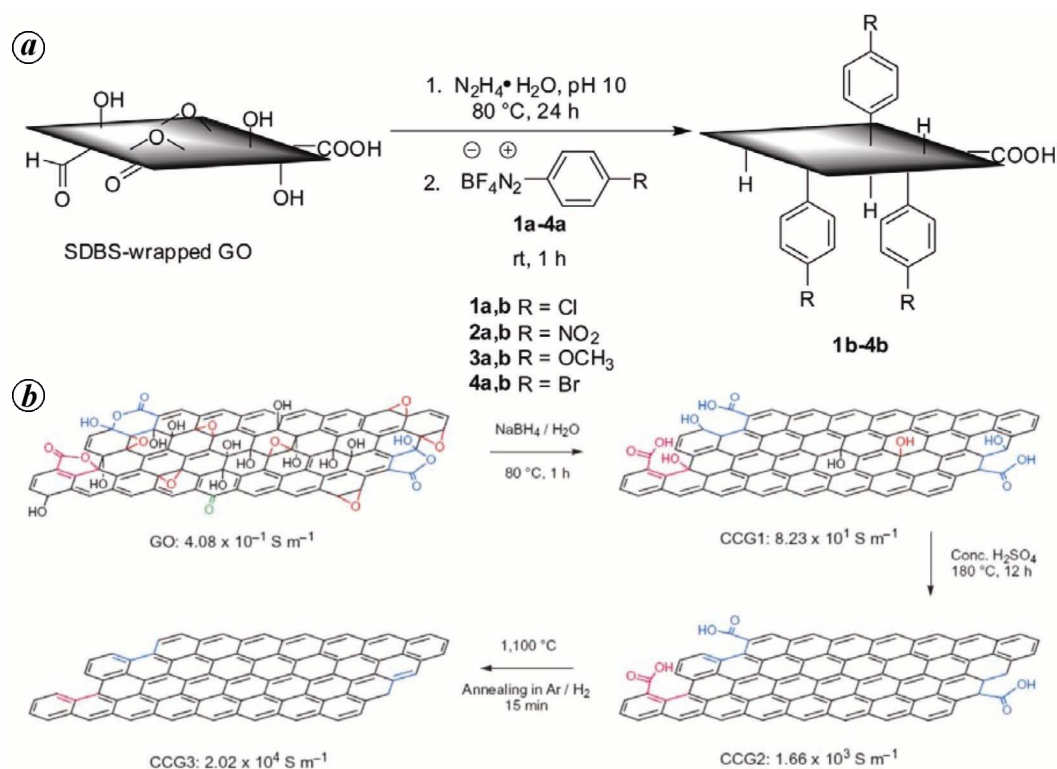


Figure 1. *a*, Hydrazine as reducing agent for the reduction of sodium dodecylbenzene sulphonate-wrapped graphene oxide, reduction and functionalization of intermediate with diazonium salts at room temperature (figure adapted from Lomeda *et al.*⁵⁹ with the permission of ACS Publications, 2008). *b*, Schematic representation of graphene oxide (GO) reduction by NaBH_4 followed by acid treatment and annealing in Ar/ H_2 (figure adapted from Gao *et al.*⁶⁷ with the permission of Nature Publishing Group, 2009).

π -conjugated structure, and leads to highly soluble and conducting graphene materials⁶⁷. Shin *et al.*⁶⁸ reported efficient reduction of graphite oxide by NaBH_4 and hydrazine (N_2H_4) and a comparison of their properties. They observed that the sheet resistance of graphite oxide film reduced using NaBH_4 is much lower than that of films reduced using N_2H_4 . Kamat and co-workers⁶⁹ studied the utility of NaBH_4 for preparing graphene–gold nanohybrids, while He and Cui *et al.*⁷⁰ reported the synthesis of dendritic platinum nanoparticles/lucigenin/reduced graphene oxide hybrid with chemiluminescence activity. They used NaBH_4 for the simultaneous reduction of H_2PtCl_4 and the lucigenin-functionalized GO (lucigenin/GO) composite⁷⁰. Chua and Pumera⁷¹ have explored the effect of three different borohydrides [sodium borohydride (NaBH_4), sodium cyanoborohydride ($\text{NaBH}_3(\text{CN})$) and sodium triacetoxymborohydride ($\text{NaBH}(\text{OAc})_3$)] in fine-tuning the oxygen composition of graphene oxides. This could be achieved due to the different substituents, which leads to variation in reducing strength. Along with hydrazine and sodium borohydride, hydroquinone has also been used as a reducing agent for the simple reduction of graphite oxide⁷² and also for the reduction of Ag^+ in silver–graphene oxide composite⁷³.

The major drawback of chemical exfoliation during oxidation of graphite to graphite oxide is the generation

of significant numbers of defects, which degrades the electronic properties of graphene. During the conversion of GO to graphene, strong chemical reducing agents like N_2H_4 and NaBH_4 are used. Such strong reducing agents are either toxic or explosive as well as difficult to handle for bulk synthesis. Thus researchers have been developing other aqueous and environment-friendly reduction methodologies for the synthesis of graphene.

Green synthetic approaches

To overcome the above said problems of strong reducing agents during chemical reduction to obtain graphene, many green strategies were developed in the past 2–3 years by researchers and will be discussed here. Contribution of Gurunathan *et al.*^{74–76} with respect to green synthesis and bioactivity-related studies of graphene, graphene oxide and their composites is noteworthy. They described the synthesis of soluble graphene utilizing biomass (*Bacillus marisflavi*) as reducing agent and studied the cytotoxic effects of graphene oxide, bacterially reduced graphene oxide (RGO) in human breast cancer cells. In their report, triethylamine (TEA) was used as reducing agent as well as stabilizer for the synthesis of biocompatible graphene. Compared to normal graphene oxide, TEA-RGO shows significantly more biocompatibility

with primary mouse embryonic fibroblast cells (PMEFs). Zhang and co-workers⁷⁷ reported simple, efficient and green method for the deoxygenation of exfoliated graphite oxide by strong alkali (NaOH or KOH, 8 M) at moderate temperatures (50–90°C; Figure 2a and b). The obtained graphene has good dispersibility in water. High-quality graphene nanosheets in a large scale without contamination of reduced material were obtained by electrochemical reduction of the exfoliated graphite oxide at a graphite electrode⁷⁸. Fabrication of nanocomposite films of platinum nanoparticle-expandable graphene sheets (Pt/EGS) on conductive indium tin oxide by electrochemical green route was done by Liu *et al.*⁷⁹. Glucose is known for its biological importance and is a mild reducing agent. Zhu *et al.*⁸⁰ developed an efficient one-pot method for the synthesis of chemically reduced graphene nanosheets from exfoliated graphite oxide in the presence of ammonia. They also compared the reactivity of glucose with other saccharides like fructose and sucrose, where similar results were obtained. An efficient, scalable, green and controllable synthetic method has been applied for the simultaneous reduction of graphene oxide and formation of Fe₃O₄ nanoparticles in a single step⁸¹. Spontaneous redox reaction of aqueous solution containing FeCl₃, K₃[Fe(CN)₆] and graphene oxide sheets results in the formation of graphene oxide sheets–Prussian blue (PB) nanocomposites. This composite shows significant sensitivity towards the electrocatalytic reduction of H₂O₂, which is higher than that of reported multiwall carbon nanotube/PB nanocomposites. This can be attributed to the novel structure of graphene oxides and the synergistic effect in the nanocomposites⁸². Iron is one of the most common elements on Earth and commercially a cheap metal. Elemental iron as reducing agent instead of harmful chemical reducing agents (Figure 2c) is being explored for the facile and green synthesis of graphene nanosheets (GNS) without any unwanted functional groups and exhibits higher absorption property for methylene blue (MB)⁸³. Similarly, Dey *et al.*⁸⁴ described the utility of elemental Zn as a reducing agent for the reduction of graphene oxide to reduced graphene oxide in acidic medium at room temperature without using any toxic reducing agent. Green tea is rich in polyphenolic compounds which are biocompatible and biodegradable. Tea polyphenols (TPs) act as reducing agents for the reduction of graphene oxide as well as a stabilizer in green tea solution for the synthesis of soluble graphene. These polyphenol–graphene can be obtained as nanofillers for the fabrication of biocomposite with chitosan⁸⁵. Zhang *et al.*⁸⁶ reported the reduction of graphene oxide sheets to water-soluble graphene in aqueous solution using ascorbic acid (AA) as reducing agent (an environment-friendly approach). AA also acts as a capping agent to stabilize RGO sheets⁸⁶. Mhamane *et al.*⁸⁷ demonstrated a single-step and green methodology for the deoxygenation of GO into water-dispersible functionalized graphene

sheets. They used the aqueous extracts of four widely distributed wild plant species and hence called the process as ‘plant extract converted graphene nanosheets (PCGN)’. The plants used for this purpose are macrophytes, namely *Potamogeton pectinatus* L. (Po), *Ceratophyllum demersum* L. (Cer) also known as Coontail or hornwort, *Lemna gibba*, (Le) and *Cyperus difformis* (Cy)⁸⁷. Thakur and Karak⁸⁸ described the reduction of graphene oxide by phytochemicals using aqueous leaf extracts of *Colocasia esculenta* and *Mesua ferrea*. Utility of super critical alcohols as reducing agent was first reported by Budi Nursanto *et al.*⁸⁹. This facile and green method involves the reduction of dispersed GO in methanol with supercritical methanol at 400°C and 300 bar for periods of 15 min to 2 h. Liu *et al.*⁹⁰ reported facile, one-pot method for the synthesis of gelatin functionalized graphene nanosheets (gelatin–GNS). Gelatin, a linear polypeptide that consists of different amounts of 18 amino acids, acts as reducing agent for the deoxygenation of exfoliated graphene oxide (EGO) and also as a functionalized reagent to prevent aggregation of graphene nanosheets. Biocompatible gelatin–GNS showed high aqueous solubility and stability in various physiological fluids. Hence this material was used to study cellular imaging and drug delivery⁹⁰. Singh *et al.*⁹¹ investigated a simple and cost-effective method for the synthesis of high-quality graphene nanosheets (GNS) directly from pencils (graphite) in ionic liquid medium. Proteins are complex amphiphilic biopolymers, featuring hydrophobic and hydrophilic groups on their surfaces, which makes them well-known for the adhesiveness to solid surfaces. Due to the presence of tyrosine (Tyr) residues, proteins such as bovine serum albumin (BSA) act as reductant. Deng and co-workers⁹² studied the interaction of BSA with GO/RGO, where BSA acts as a stabilizer as well as a decorating agent in obtaining BSA–GO/RGO conjugate. At suitable pH and temperature, reaction between BSA–GO/RGO conjugate and pre-synthesized metal nanoparticles produces graphene–metal nanoparticle (metal = Au, Pt, Pd, Ag, etc.) assemblies⁹² (Figure 3). Zinc is an amphoteric metal which can react both in acidic and basic conditions. Liu *et al.*⁹³ established a short-time processing method for the synthesis of graphene nanosheets by Zn reduction at room temperature and under mild alkaline conditions (can be called as a green method). The Zn–GO-based primary batteries thus prepared in the presence of aqueous KOH electrolyte solution⁹³ show maximum specific capacitance of 116 F/g. Tannic acid (TA), widely present in wood, is a water-soluble, phenolic hydroxyl-rich compound which acts as a reducing agent. Zhang *et al.*⁹⁴ explored the utility of TA for the reduction of AgNO₃ and GO in making AgNPs–graphene nanocomposite. This is a simple, cost-effective and one-pot method. The resultant AgNPs–G nanocomposites show excellent surface enhanced Raman scattering (SERS) activity as SERS substrates, for H₂O₂ reduction and also glucose

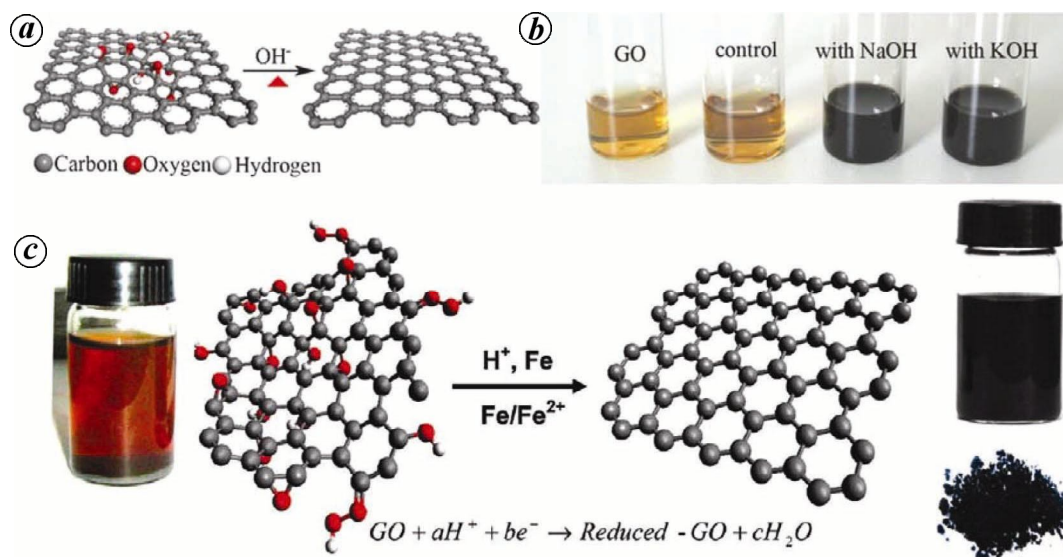


Figure 2. *a*, Equation showing the deoxygenation of exfoliated GO in the presence of base. *b*, Images of the exfoliated-GO suspension before and after addition of base; change in colour is observed. (*a*) and (*b*) adapted from Fan *et al.*⁷⁷ with the permission of John Wiley and Sons, 2008. *c*, Iron as a reducing agent for the preparation of graphene nanosheets GNS under acidic condition. Reproduced with the permission from Fan *et al.*⁸³ with the permission of ACS Publications, 2011.

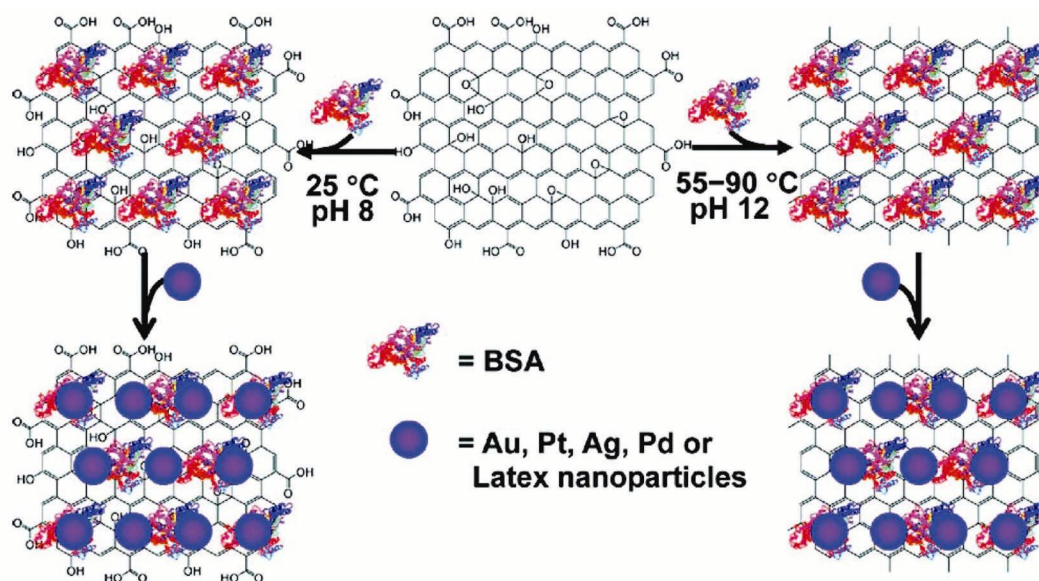


Figure 3. Illustration of GO reduction to RGO by bovine serum albumin (BSA) and its composite with metal leading to a general nanopatform for nanoparticle assembly. Reproduced with the permission from Liu *et al.*⁹² with the permission of ACS Publications, 2010.

detection in both buffer and human blood serum⁹⁴. L-Cysteine is an interesting amino acid that contains three functional groups ($-\text{SH}$, $-\text{NH}_2$ and $-\text{COOH}$) and it acts as reducing agent, sulphur donor and as a linker. H_2S is released when L-cysteine is heated and it is used for the reduction of GO to RGO. L-Cysteine acts as a linker to anchor Cu^{2+} for the growth of the CuS nanoparticles on the RGO sheets. CuS/RGO nanocomposites show enhanced photocurrent response and improved photocatalytic activity in the degradation of methylene blue compared to pure CuS. This was attributed to the efficient

charge transport of RGO sheets and hence reduced recombination rate of excited carriers⁹⁵. Yoo and co-workers⁹⁶ reported facile and robust one-step synthesis (green) of TiO_2 -graphene composite and investigated its performance in photocatalytic applications. The catalysts show enhanced photocatalytic activity towards the degradation of rhodamine B dye and benzoic acid under visible light irradiation⁹⁶. Pradeep and co-workers⁹⁷ reported the synthesis of graphene from cane sugar (green process). Without using any binder, graphene was immobilized on sand to make graphene sand composite (GSC). GSC

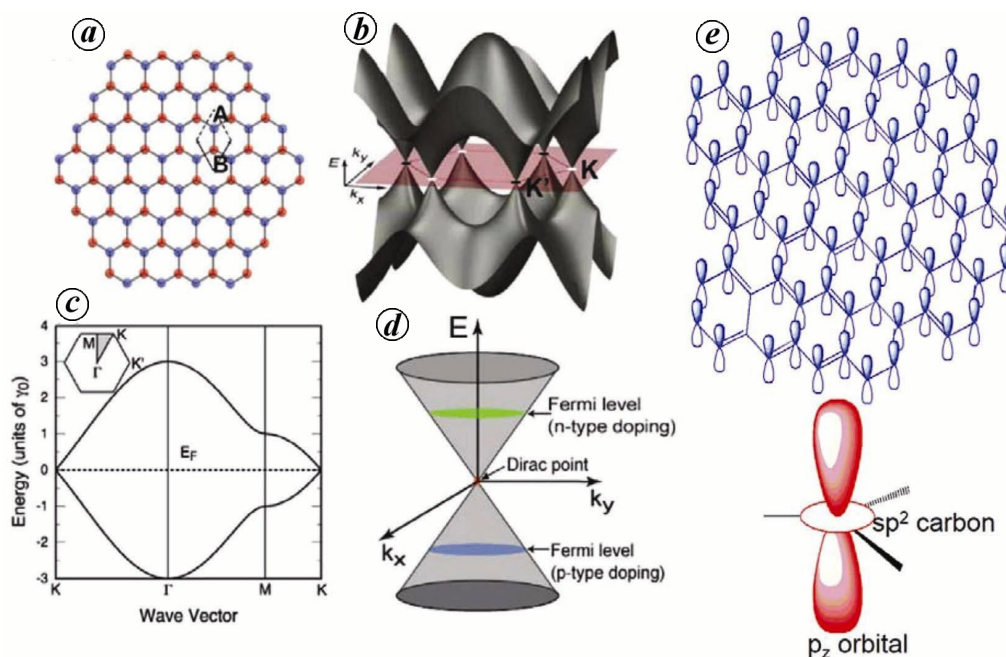


Figure 4. *a*, Two atoms (A (blue) and B (red)) per unit cell in hexagonal honeycomb lattice of graphene. *b*, The three-dimensional band structure of graphene. *c*, Energy vs k -space diagram of graphene. *d*, Low-energy diagram at Dirac point and Fermi-level position for different doping. *e*, Schematic of the graphene π - π delocalization and singly occupied p_z orbital in sp^2 hybridized carbon. ((*a*–*d*) have been adapted from Avouris¹⁷ with the permission of ACS publications, 2010).

obtained from this simple and cost effective method was utilized for water purification⁹⁷. Chen *et al.*⁹⁸ reported a nontoxic, rapid, one-pot and template-free synthesis of monodisperse Pt nanoflowers (PtNFs) supported on graphene oxide nanosheets using low-cost ethanol (green solvent) as reducing agent. The resulting PtNFs–GO hybrids were found to exhibit distinctly superior electrocatalytic activities towards methanol oxidation⁹⁸. Sui *et al.*⁹⁹ reported the fabrication of ultralight graphene–CNT hybrid aerogel from aqueous gel precursors (graphene oxide and carbon nanotubes) with vitamin C processed by supercritical CO₂ drying (an efficient and green method). The resulting hybrid aerogels show promising performance in water purification, including capacitive deionization of light metal salts, removal of organic dyes and enrichment of heavy metal ions⁹⁹. Zhang *et al.*¹⁰⁰ developed a low-cost, fast, facile and green method using ultrasound assisted approach for the controlled synthesis of Cu₂O–graphene hybrid nanomaterials. Cu(OAc)₂, glucose and ethylene glycol (EG)-coated graphene oxide were mixed together followed by ultrasound treatment. The Cu₂O–graphene hybrid material when used as an anode exhibited enhanced performance¹⁰⁰. For a lithium ion battery, different concentrations of silver ion and different reaction times result in various morphologies like nanospheres, nanocubes and dendrites on graphene oxide. Wang *et al.*¹⁰¹ reported a one-pot solution-phase (green) synthetic method without using any reducing agent or surfactant for the synthesis of Pt/CeO₂/graphene

nanomaterials. L-Lysine is used as a linker and graphene oxide as oxidant to oxidize Ce³⁺ into CeO₂ NPs. The obtained Pt/CeO₂/graphene composites are used for the electrocatalytic oxidation of methanol, which shows better catalytic activity than simple Pt/graphene and commercial Pt/C catalysts. Graphene oxide–silver hybrids synthesized via spontaneous reduction have great potential in applications such as ultrasensitive detection of biomarkers, SERS enhancement and as electronic chemical sensors in the near future¹⁰². Heparin is a natural polymer material with excellent biocompatibility and is used as an anticoagulant. Huang and co-workers¹⁰³ used a simple (green) method for heparin-functionalized RGO, wherein heparin acts both as reducing agent and stabilizer. The heparin–RGO hybrid has a potentially wide range of uses in the biomedical field, such as for the treatment of thrombosis¹⁰³. The simultaneous reduction of metal salts and GO by focused solar radiation results in a novel hybrid composite composed of 2D graphene and 3D magnetic/nonmagnetic/metal/metal oxide nanoparticles. The evenly deposited metal/metal oxide nanoparticles dispersed graphene composites have potential applications in energy storage and conversion devices, heterogeneous catalysis and sensing¹⁰⁴.

Electronic properties

Electronic behaviour of graphene is unlike a semiconductor¹⁰⁵, where there is no band gap as the conduction band

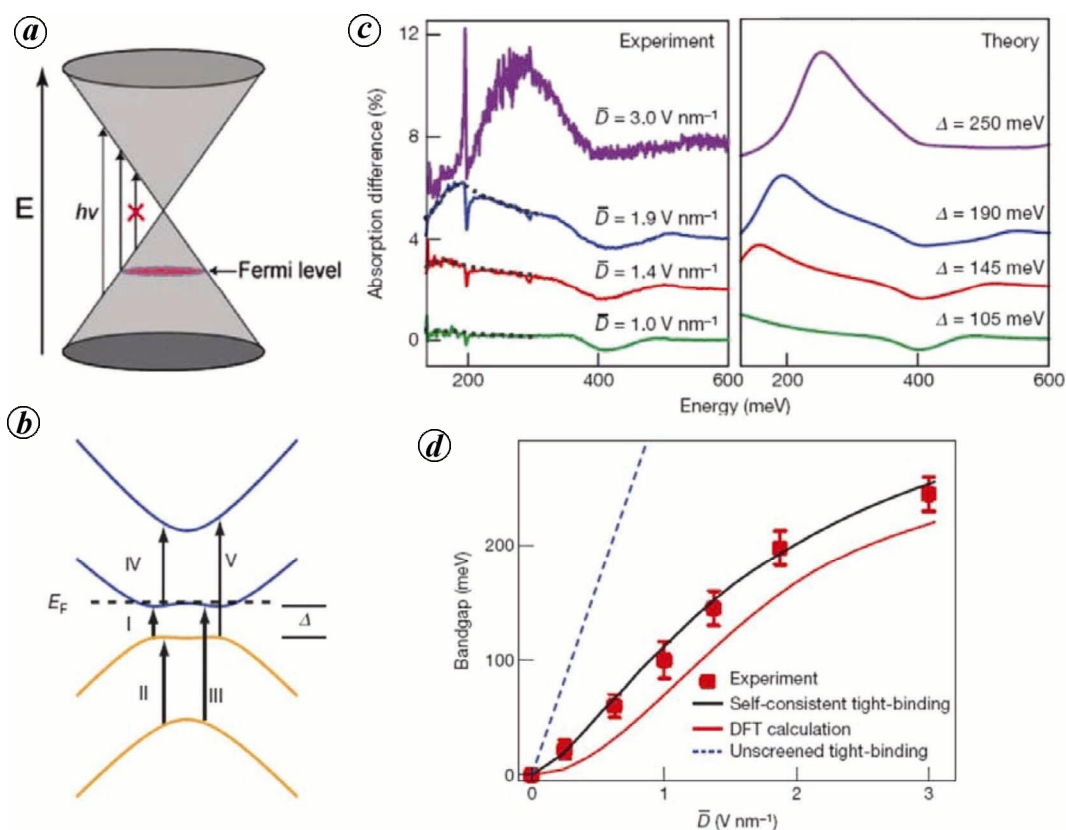


Figure 5. *a*, Optical transitions in a doped single-layer graphene (allowed condition $E_{hv} > 2\Delta(E_F - E_{Dirac})$); adapted from Avouris¹⁷ with the permission of ACS Publications, 2010). *b*, Allowed optical transitions in different sub-bands of bilayer graphene. *c*, Experimental and theoretical absorption spectra at charge neutral point varying displacement fields \bar{D} . Transition *I* (peak below 200 meV) is the gate-induced band gap (dashed black lines). Electronic transitions II–V are responsible for the broad feature around 400 meV. *d*, Experimental and theoretical band gap dependent on the electric-field in bilayer graphene. (*b*–*d*) have been adapted from Zhang *et al.*¹⁰⁹ with the permission of Nature Publishing Group, 2009.

and valence band touch each other at the six Dirac points (K and K' in Brillouin zone)¹⁷ (Figure 4). Electrons in graphene behave like massless particles and can be called as 2D Dirac electrons. The bonding between carbon atoms is the combination of two sp^2 hybridized orbitals separated by 1.42 Å, which leads to the planar morphology of graphene (Figure 4e). According to Pauli's principle, half-filled perpendicular p-orbitals overlap to form π -bonds between two carbon atoms. The π -electrons, conjugated throughout the graphene surface, contribute to the conduction as found in graphene.

Functionalization of the sp^2 hybridized carbon atom of graphene leads to formation of sp^3 carbon, which creates defect sites in the graphene structure leading to the removal of π -electrons¹⁰⁶. This π -electron removal (covalent functionalization) can generate a band gap in graphene. Sreepasad and Berry¹⁰⁶ discussed the change in carrier mobility (from 20,000 to 0.05–200 cm² V⁻¹ s⁻¹) in reduced graphene oxide (RGO) due to the presence of residual oxy groups changing the properties of graphene to a *p*-type semiconductor with a band gap of 0.2 to 2 eV. Similarly, oxygen attachment to graphene (via bridging O or epoxy form) changes the s-character of hybridization

and thus disrupts the C–C bond symmetry, thereby generating three LUMO levels with maximum gap of 0.64 eV, instead of pristine LUMO level¹⁰⁷. Chen *et al.*¹⁰⁸ reported that the semiconductor property of graphene oxide can be *p*- or *n*-type. In conjugation with TiO₂, graphene oxide has a band gap narrower than 2.43 eV; the *p*-type form acts as a sensitizer and has significant effect on visible light photocatalysis, whereas the *n*-type form has a negligible effect. The allowed optical transitions (Figure 5a) in a doped single-layer graphene can be observed¹⁷ only when $h\nu > 2\Delta(E_F - E_{Dirac})$. The allowed optical transitions in bilayer graphene have been experimentally shown¹⁰⁹ as a gate-controlled, tunable band gap opening in bilayer graphene up to 250 meV. Electric gating in the presence of applied electrical displacement field is responsible for the shift in the Fermi level, breaking the inversion symmetry at the Dirac points in bilayer graphene and resulting in the band gap of bilayer graphene. The experimental absorption peaks due to gate-induced band-gap opening were fitted using tight binding model (Figure 5b)¹⁰⁹. Samarakoon and Wang¹¹⁰ theoretically investigated the continuous tunable band gap in biased bilayer graphene upon hydrogenation, which transforms sp^2 carbon to sp^3

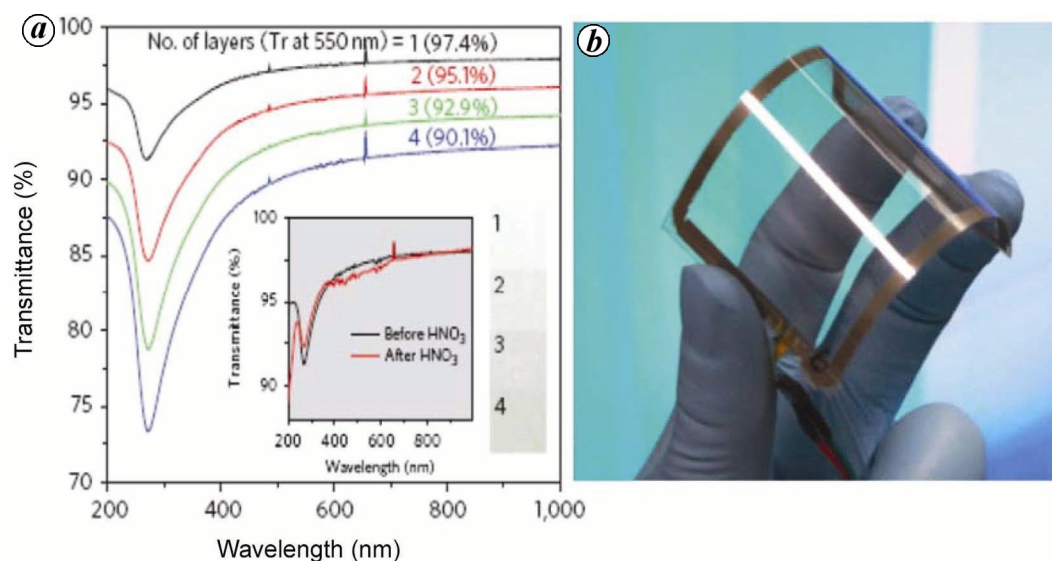


Figure 6. *a*, UV-Vis spectra of roll-to-roll layer-by-layer transferred graphene films on quartz substrates. (Inset) UV spectra of graphene films with and without HNO₃ doping. Optical images for the corresponding number of transferred layers (1 × 1 cm²). *b*, Optically transparent and flexible graphene-PET film (figure adapted from Bal *et al.*¹⁹ with the permission of Nature Publishing Group, 2010).

carbon. Coupling with Si islands, graphene shows a band gap opening up to 3.2 meV (with 10 atom % Si)¹¹¹.

Electronic properties of graphene are also dependent on the doping like N, S, B, etc. B-doped and N-doped graphene behaves like p-type and n-type semiconductors respectively, and the electronic properties depend on the amount of doping^{112,113}. Panchakarla *et al.*¹¹³ have discussed a remarkable result on band opening in monolayer graphene, whereas a weak quadratic dispersion was observed in bilayer graphene on doping.

Optical properties

Besides electronic properties, graphene is a very good optical material due to its π -electron cloud (puddle) formation, very low optical reflectivity and high optical transmittance. Due to its unique electronic structure, single-layer graphene has 97.4% optical transmittance (Figure 6) and it decreases linearly with the number of layers¹⁹. Light transmittance through free-standing graphene sheets is given by $T = (1 + \pi\alpha/2)^{-2} \approx 1 - \pi\alpha \approx 0.977$, where T is the transmittance and α is the fine structure constant¹⁷. Kim *et al.*¹¹⁴ demonstrated efficient electrically controlled plasmon resonance in graphene due to its strong and tunable interband transitions. Propagating optical plasmons in tapered graphene has been observed with IR excitation using near-field scattering microscopy¹¹⁵. Wide spectrum tunable luminescence property of graphene and its derivatives has great impact on graphene-based technologies. Graphene-based hybrid materials are important for luminescence properties, as graphene shows very weak luminescence. Graphene

quantum dots (GQDs) are nano-sized sheets of carbon atoms which show strong tunable photoluminescence due to surface effect¹¹⁶. Zhu *et al.*¹¹⁷ have synthesized green fluorescent GQDs (diameter of ~ 5.3 nm) which absorb at 320 nm and show strong photoluminescence (PL) at 515 nm with 11.4% quantum yield. Shinde and Pillai¹¹⁸ have synthesized size-tunable spherical GQDs via electrochemically lateral unzipping of multi-walled CNTs. They have discussed the photophysical¹¹⁸ and different redox properties¹¹⁹ of these size-tunable narrow band gap semiconductors (GQDs).

Photocatalytic properties

Recently, significant attention has been given to the application of graphene-based hybrid materials in photo-electrochemistry in areas like electrochemical solar cells, photocatalytic degradation of organic pollutants, water splitting for hydrogen evolution, photocatalytic conversion of fuels, etc. based on graphene-based hybrid materials with semiconducting properties. An electron transition from valence band to conduction band in semiconductors upon excitation by a photon ($E \geq E_g$) generates an exciton pair (an electron in conduction band and a positive hole in the valence band).

These excitons move to the catalytic active sites of the semiconductor, where the electron reduces and the hole oxidizes the reactants. The basic mechanisms of photocatalytic organic pollutant degradation, photocatalytic H₂ evolution, photocatalytic fuel conversion and photovoltaics are involved with these oxidation and reduction processes. Significant work has been carried out for

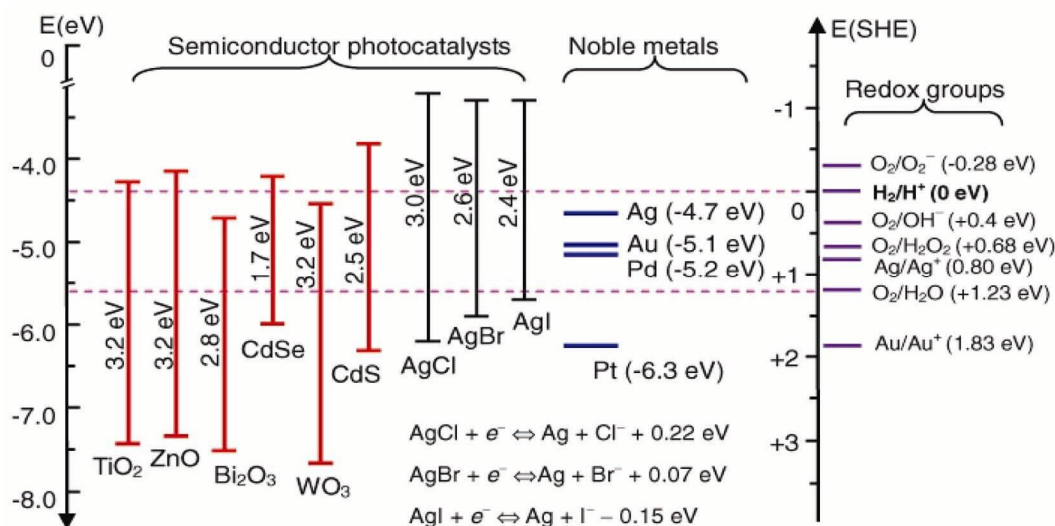


Figure 7. Electronic band gap and band potentials of different semiconductors and metals (figure adapted from Zhang *et al.*¹⁹⁵ with the permission of IOP Publishing, 2013).

obtaining efficient photocatalysts by tuning the structure, morphology, size, composites and hetero-junctions of materials such as TiO₂, Ta₂O₅, ZnO, ZnS, Bi₂WO₆, WO₃, NaTaO₃, Fe₂O₃ and CdS. Factors such as (i) recombination of the excitons, (ii) efficient solar light absorption and (iii) effective conversion of the solar light towards photocatalysis (not in the form of phonons or heat) are the key aspects on which research is still being pursued to control the photocatalytic efficiency of the semiconductor. Low band gap materials are effective to absorb solar light, where reflections or scattering of light can be reduced.

The photoelectrochemical performance and the visible light absorption by the semiconductor materials have been improved by different metal-ion doping, anion doping, adding hole scavengers (electron donors), creating oxygen vacancies, adding co-catalyst, loading noble metal particles, dye sensitization and forming composite semiconductors. Excellent absorptivity, transparency, conductivity, nontoxicity, diverse functionalities and controllability of graphene lead to its super photoelectrochemical performance by making its hybrids with semiconductors.

The band gap and band potentials of the semiconductors are important for the particular type of photocatalytic process, as depicted in Figure 7. Graphene is considered to be an outstanding candidate for the hybrid photocatalytic material¹²⁰ as it has the work function around -4.4 eV, whereas semiconductor nanostructures have their conduction band position at around -3.5 eV (vacuum level; Figure 7). This helps in the photogenerated electron transfer process from conduction band of the semiconductor to graphene surface¹²¹. The exciton recombination gets delayed due to the delocalization of the photogenerated electron on graphene surface. Graphene in nanocom-

posite photocatalytic materials also plays an important role by increasing the solar light absorption efficiency. Graphene also decreases the band gap of the semiconductors leading to an efficient solar light absorber. For example, TiO₂ (P25) nanoparticles are active in UV light¹²²; however, they become effective visible light catalyst in conjugation with graphene. ZnS nanoparticles extend their absorption edge towards the visible range in conjugation with graphene¹²³. BiOBr nanoparticles conjugated to graphene have lowered indirect band gap than that of pure BiOBr material¹²⁴. In addition, graphene having high surface area provides sufficient space for the adsorption of organic pollutants¹²⁵, which is one of the key factors for heterogeneous photocatalysis.

Metal oxides like TiO₂ (ref. 126) and ZnO (ref. 127) are wide band gap materials showing high photocatalytic efficiency under UV light. Graphene oxide can be hybridized easily with these metal oxides via electrostatic interaction between metal ions and oxide groups (mainly hydroxyl, carboxyl or epoxy groups) in graphene. Sometimes semiconductor particles such as TiO₂ (refs 122, 128), Ta₂O₅ and BiOBr (ref. 124) have been conjugated with graphene oxide directly via electrostatic interactions. The interfacial charge transfer (IFCT) at the graphene-semiconductors plays the most important role for enhancing the photocatalytic efficiency as documented in the case of graphene-TiO₂ system, where IFCT takes place through chemically bonded (C-Ti) interfacial contact¹²⁹. This IFCT has been experimentally verified using electrochemical impedance spectroscopy (EIS), the gaseous phase photocurrent and photoluminescence studies (Figure 8)¹²⁹, which decreases the recombination of the excitons, thereby enhancing the photocatalytic efficiency. Similarly, exciton recombination in metal sulphides such as ZnS, CdS and Bi₂S₃ has been delayed by introducing

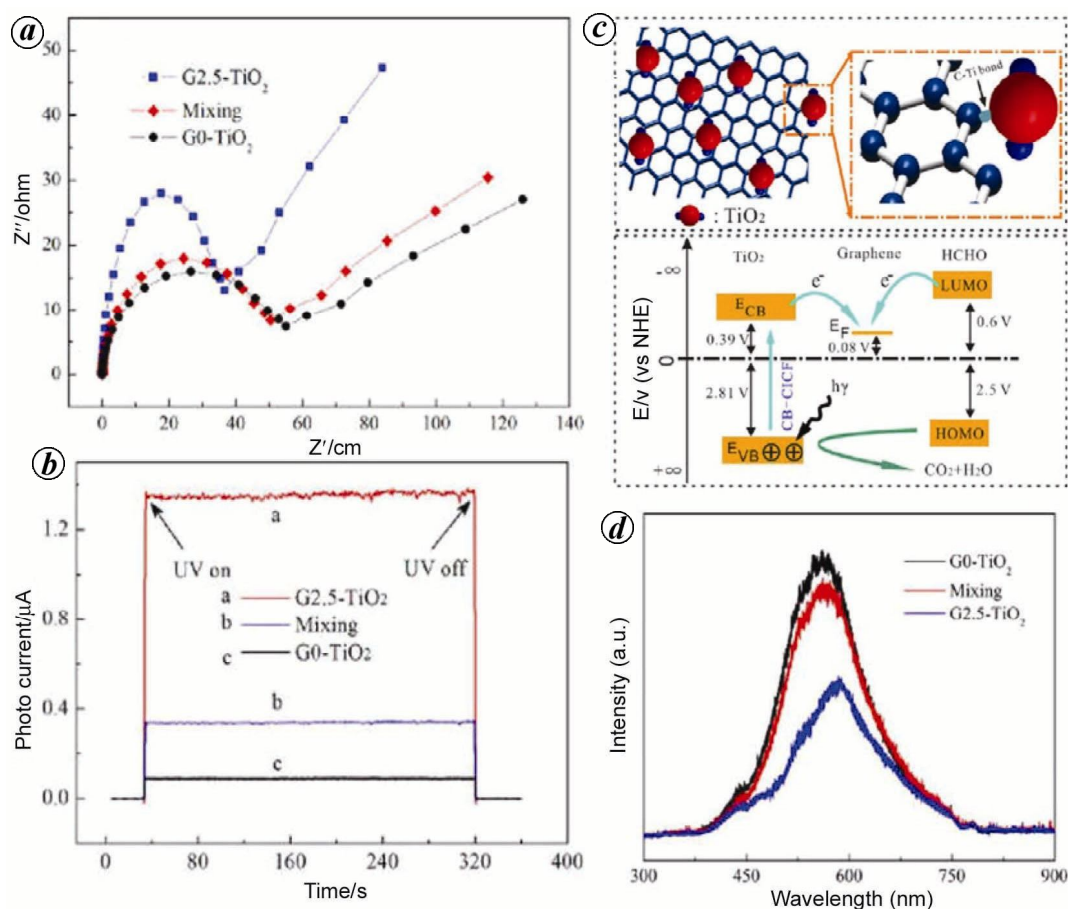


Figure 8. *a*, EIS spectra; *b*, Gaseous phase photocurrent of graphene–TiO₂ samples. *c*, Schematic of interfacial charge transfer (IFCT) in graphene–TiO₂ samples. *d*, PL emission spectra of graphene–TiO₂ samples. (Figures have been reproduced from Huang *et al.*¹²⁹ with the permission of ACS Publications, 2013.)

graphene¹²³. The photocatalytic performance of few graphene-based composites has been listed in Table 1.

To get higher photocatalytic efficiency or for smart photocatalysts, a design of ternary catalysts based on graphene such as graphene–Ag@AgBr (ref. 130), graphene–Ag@AgCl (ref. 131), graphene–CdS–Pt (ref. 132) and graphene–TiO₂–MoS₂ (ref. 133) has been explored.

Energy storage

Lithium-ion batteries

Increasing demand of mobile technology, highly efficient, low-cost, environmentally green energy storage devices in the form of rechargeable batteries or capacitors are important for current generation. Graphene and its hybrids have high potential for their energy storage properties as they have extraordinary high surface area⁶, high conductivity and high flexibility. Lithium ion batteries (LIBs) work by the intercalation of Li⁺ in the cathode materials and upon charging, Li⁺ ions released from the cathode, intercalate into the anode material forming alloy

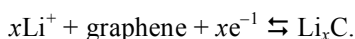
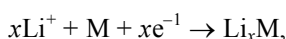
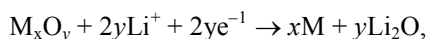
structures or Li/C. The reverse process takes place upon discharging. In terms of volumetric density, coulombic efficiency (ratio of extracted Li⁺ to inserted Li⁺), safety and life cycle, graphene-based hybrid materials are of great choice for LIBs. Graphene is advantageous due to its high coulombic efficiency and reversible charge–discharge process at low potential. Sheet morphology and large surface area of graphene increase the interface for Li⁺ ion interactions. Graphene provides good 2D platform for active materials in graphene-based hybrid materials¹³⁴. A maximum capacity of 372 mAh g^{−1} for graphite can be obtained as one Li⁺ ion can be accommodated by one six-member carbon ring in graphite, forming a composition of LiC₆. In single-layer graphene, both the sides of the ring can host Li⁺ ion giving the maximum Li-intercalation during charging to two Li per six-member carbon ring (Li₂C₆), which provides a maximum capacity of 744 mAh g^{−1} (theoretical)¹³⁴.

In composite materials, several metal oxides like TiO₂ (ref. 135), MnO₂, CoO, NiO, VO₂ (refs 136 and 137), V₂O₅, LiMn₂O₄, LiCoO₂, SnO₂ (refs 138–145), Co₃O₄ (ref. 146), Fe₃O₄ (ref. 147), etc. are hybridized with

Table 1. Photocatalytic performance of different graphene-based hybrid materials

System	Morphology	Band gap	Reaction	Light source	Dye degradation rate or efficiency	Reference
Graphene-TiO ₂ (P25)	Spherical	P25: 3.18 eV G-P25: 2.9 eV	Degradation of methylene blue	UV and visible light	UV: ~85% in 55 min Bare P25: ~25% in 55 min Vis: ~65% in 65 min Bare P25: 12% in 65 min	122
Graphene-TiO ₂	Spherical	–	RhB degradation	300 W Xe lamp	G-TiO ₂ : ~99% in 30 min TiO ₂ : ~30% in 30 min	135
Graphene-TiO ₂	Nanotube	–	Degradation of malachite green	Mercury lamp	G-TNT: 0.0674 min ⁻¹ , TNTs: 0.0218 min ⁻¹	196
Graphydyne-TiO ₂ Graphene-TiO ₂	Particles	–	Methylene blue degradation	Xe lamp Solar light simulator	Graphydyne-TiO ₂ : 0.0247 min ⁻¹ Graphene-TiO ₂ : 0.0195 min ⁻¹ Pure TiO ₂ : 0.0152 min ⁻¹	197
Graphene-BiOBr	Nanoplates	Indirect band gap Pure BiOBr: 2.81 eV G-BiOBr: 2.58 eV	Rhodamine B degradation	Visible-light irradiation	0.132 min ⁻¹ 0.042 min ⁻¹ (control)	124
Graphene-g-C ₃ N ₄	Layered composite	2.7 eV No change in band gap	H ₂ evolution degradation	UV cut-off Xe arc lamp	Pure g-C ₃ N ₄ 147 μmol h ⁻¹ g ⁻¹ G-gC ₃ N ₄ composite 451 μmol h ⁻¹ g ⁻¹	198
Graphene-ZnS	Spherical particles	–	Methyl orange degradation	300 W mercury lamp	ZnS: 0.00609 min ⁻¹ , G-ZnS: 0.02558 min ⁻¹	123
Graphene-CdS	Very small (~10 nm) particles	–	Methyl orange degradation	300 W mercury lamp	CdS: 0.00481 min ⁻¹ , G-CdS: 0.01362 min ⁻¹	123
Graphene-Bi ₂ S ₃	Aggregated nanoparticles	–	Methyl orange degradation	300 W mercury lamp	Bi ₂ S ₃ : 0.00734 min ⁻¹ G-Bi ₂ S ₃ : 0.01204 min ⁻¹	123
ZnO _{1-x} /graphene	Graphene-coated particles	~3.02 eV	Methylene blue degradation	Visible and UV light	Visible: 0.60 h ⁻¹ UV light: 0.19 min ⁻¹	199

graphene as a anode material for LIBs. The basic mechanism of LIBs is as follows¹⁴⁸



Supercapacitors

Supercapacitors are the electrochemical devices which store and release energy at high rate, high power density and have longer life cycles than batteries¹⁸. Carbon-based materials having high surface area and good conductivity

such as graphene and graphene-like carbon sheets are more important for their good electrochemical double-layer capacitor (EDLC) properties, where charge accumulation takes place at the electrode-electrolyte interface. Graphene-based supercapacitors follow the electrochemical double layer capacitance mechanism. In 1997, Niu *et al.*¹⁴⁹ studied the supercapacitance properties in CNTs, while Ruoff and his group¹⁵⁰ are the pioneers to study the supercapacitance of chemically modified graphene which has been denoted as an ultracapacitor. In 2011, the above group investigated¹⁵¹ the electrical double layer capacitance in activated graphene having very high surface area (up to 3100 m²/g). A new method was developed based on laser reduction using normal LightScribe DVD drive by El-Kady *et al.*¹³ to obtain highly conducting (1738 S/m) reduced graphene oxide having high

surface area ($1520 \text{ m}^2/\text{g}$). Being highly conducting and having a two-dimensional platform with large surface area, graphene is the ideal system for making hybrids for better supercapacitors with high energy density and high power density. These laser-reduced graphene films have been studied as a binder or current collector free electrochemical capacitors and have ultrahigh energy and high power density¹³. A very high energy density of 85.6 Wh/kg at 1 A/g at room temperature (or 136 Wh/kg at 80°C) in graphene-based supercapacitor has been reported by Liu *et al.*¹⁵², where restacking of graphene sheets got restricted as these mesoporous graphenes are curved. Wu *et al.*¹⁵³ have focused on the composites of graphene and polyaniline nanofibres which are sandwiched between graphene layers. These composites having very good conductivity (550 S/m) and flexibility, showed large specific capacitance of 210 F/g at a discharge rate of 0.3 A/g (ref. 153). Mishra and Ramaprabhu¹⁵⁴ studied hydrogen-induced exfoliation of graphene and its composite formation with metal oxides (RuO_2 , TiO_2 and Fe_3O_4) and polyaniline. The supercapacitance of the device has three contributions: (i) electrochemical double layer capacitance, where it adsorbs both anions and cations to store energy; (ii) pseudo-capacitance, where it involves fast and reversible redox reactions and stores energy via Faradaic processes, and (iii) asymmetric capacitance, where one is Faradaic electrode and the other is capacitive electrode¹⁵⁵. Several studies on graphene-based hybrids of metal oxides, sulphides and hydroxides (graphene- TiO_2 , graphene- V_2O_5 , graphene- VO_2 , graphene- $\text{Ni}(\text{OH})_2$, graphene- $\text{Co}(\text{OH})_2$, graphene- NiCo_2O_4 , graphene- MoS_2 , graphene- WS_2 , graphene- CoO , Graphene- MnO_2 , graphene- MnO) have been reported to understand the supercapacitor properties and the underlying mechanism.

Energy and electronic applications

Recently, graphene has been applied in several ways related to energy and electronics. In energy-related application, graphene-based anode systems were used as they need less time to recharge than usual LIBs. Graphene-based materials have the power to store electrons in the form of electrical energy as LIBs, whereas it required minutes to recharge instead of hours. Graphene has been used for low-cost, more efficient solar cells and fuel cells. In electronics, low-cost, easily recyclable, display screens have been developed using graphene instead of indium-based electrode in OLED. Field effect transistor (FET) and high-frequency transistors have also been developed based on graphene, as electrons can move much faster on graphene compared to silicon. Graphene-based antennas and transceivers have been developed for communication between nanomachines in electronics.

Application in water desalination

The development of modern industry and increase in population growth globally led to freshwater shortage. Desalination is one alternative for producing potable freshwater from brackish/sea water. Reverse osmosis (RO), thermal processes, electro dialysis and ion exchange are the widely used technologies for desalination. However, these technologies are energy- and capital-intensive. Capacitive deionization (CDI) is a novel water purification technology without any secondary pollution¹⁵⁶. This involves absorption of ionic species onto the charged porous electrode. Several materials such as carbon aerogels^{157,158} activated carbon (AC)^{159,160} mesoporous carbon (MC)^{161,162} carbon nanotubes (CNTs)¹⁶³ and carbon composites¹⁶⁴ are investigated as electrodes in CDI technology. Graphene exhibits large specific surface area, high electric conductivity, remarkable mechanical flexibility and good chemical inertia⁴⁴. With respect to the excellent physical, chemical and mechanical properties, graphene has emerged as a desirable electrode for energy storage as well as electrosorption. Pradeep and co-workers¹⁶⁵ proposed a simple strategy for the RT synthesis of RGO-composites with silver, gold and MnO_2 . They studied the utility of RGO-Ag and RGO- MnO_2 for removing heavy metals from water¹⁶⁵.

Wimalasiri *et al.*¹⁶⁶ studied the synthesis and applications of carbon nanotube/graphene (CNT/G) composite as electrodes for capacitive deionization (CDI), which exhibits a specific capacitance of 220 F/g and an electrosorption capacity of 26.42 mg/g with 100% regeneration, showing great potential as a high-performance electrode material in CDI applications.

Wang *et al.*¹⁶⁷ reported the synthesis of reduced graphene oxide resol composite (RGO-R) as electrodes for CDI. The addition of resol enhances the specific surface area of RGO, which results in high NaCl uptake. The equilibrium electrosorption capacity and rate constant increased with the voltage at 1.5 V as 1.00234 mg/g and 0.05394 min^{-1} respectively. Compared with AC and the as-synthesized RGO, this RGO-R material can be a suitable candidate for electrodes, which shows promising potential for efficient CDI process in brackish water desalination and drinking water purification¹⁶⁷.

Wen *et al.*¹⁶⁸ prepared graphene-based hierarchically porous 3D carbon (3DGHPC) by a dual template strategy and explored its electrode performance for CDI. 3DGHPC presents a higher electrosorption capacity of 6.18 mg g^{-1} and an increased desalination efficiency of 88.96%. The increased surface area ($384.4 \text{ m}^2 \text{ g}^{-1}$) and pore volume ($0.73 \text{ cm}^3 \text{ g}^{-1}$) of 3DGHPC compared to 3D graphene are responsible for its better electrode performance¹⁶⁸.

Sint *et al.*¹⁶⁹ designed functionalized nanopores in graphene monolayers using MD simulations and showed that they could serve as ionic sieves of high selectivity

and transparency. The F–N-pore is terminated by negatively charged nitrogen and fluorine, favouring the passage of cations, whereas H-pore is terminated by positively charged hydrogen, favouring the passage of anions¹⁶⁹. Zhao *et al.*¹⁷⁰ prepared graphene sponges (GSs) by hydrothermal treatment using thiourea. These GSs show a tunable pore structure, surface properties and high adsorption ability for various types of water contaminations¹⁷⁰.

Presence of arsenic in drinking water is a serious problem in South Asia. Chandra *et al.*¹⁷¹ reported the synthesis of magnetite–RGO (M–RGO) hybrid which is superparamagnetic and shows very high binding capacity for As(III) and As(V). They also prepared 5–20 wt% GO-loaded polypyrrole (Ppy), (PPy–RGO) composite which shows highly selective and enhanced adsorption of Hg²⁺ for environmental cleaning¹⁷².

Zhu *et al.*¹⁷³ reported the synthesis of magnetic graphene nanocomposites (MGNCs) decorated with core@double-shell crystalline NPs, which are composed of crystalline iron core, iron-oxide inner shell and amorphous SiO₂ outer shell. The MGNCs demonstrate an extremely fast Cr(VI) removal from the wastewater with a high removal efficiency and with an almost complete removal of Cr(VI) within 5 min. The adsorption kinetics follows the pseudo second-order model and the novel MGNC adsorbent exhibits better Cr(VI) removal efficiency in solutions with low pH¹⁷³. Wang *et al.*¹⁷⁴ reported a facile method for the preparation of magnetic mesoporous silica–graphene oxide (MMSP–GO) composites and investigated the synergistic adsorption of humic acid (HA) and heavy metal ions, specifically Pb(II) and Cd(II). Among the graphene-based composites, chitosan grafted with GO sheets conjugated with magnetic particles as adsorbent for Pb²⁺ ions¹⁷⁵, calcium alginate with encapsulated GO gel beads¹⁷⁶ for Cu²⁺, iron-based adsorbents¹⁷⁷ for Zn²⁺ and graphene oxide cross-linked with ferric hydroxide for arsenate¹⁷⁸ are studied for the removal of these ions from wastewater.

Biological and medical applications

Graphene and graphene-based composites having very high surface area and biocompatibility are important for drug loading and bio-conjugation. They have been used as nano carriers for drug and gene delivery. Graphene having absorbance in NIR has been used for photothermal therapy. Different inorganic nanoparticles (Au, Ag, Pt, Cu, Fe₃O₄, QDs, ZnO, SiO₂, TiO₂, etc.) decorated on graphene are useful for multimodal imaging and therapeutic applications. Graphene and graphene composites having very high surface area can have significant biomolecular interactions via π – π interactions for antibacterial applications, drug delivery, gene transfection, tissue scaffolds and biosensing.

Graphene–Fe₃O₄ conjugates have good magnetic and optical properties and are used in biomedicine. Recently, Fan *et al.*¹⁷⁹ proposed a novel nanocarrier based on Fe₃O₄–graphene nanocomposite for effective drug delivery and pH-responsive release system for cancer treatment. These composites exhibit excellent biocompatibility and have synergic effect of both superparamagnetic property of Fe₃O₄ and water solubility of nano-graphene. Graphene–Fe₃O₄ composites could be used as contrast agent for MRI applications. Yang *et al.*¹⁸⁰ reported hybrids of superparamagnetic graphene oxide–Fe₃O₄ nanoparticles (GO–Fe₃O₄) prepared via simple chemical precipitation method, where 18.6 wt% Fe₃O₄ was loaded on graphene sheet; the hybrid material has the drug (doxorubicin hydrochloride) loading capacity around 1.08 mg per mg of the hybrid material. Graphene–PEG–Fe₃O₄ hybrid has been studied for applications *in vivo* on magnetic resonance imaging (MRI) and localized photothermal therapy of magnetically guided cancer cells¹⁸¹.

A promising MRI T_2 contrast agent, graphene oxide decorated with MnFe₂O₄ nanoparticles was prepared through a simple mini-emulsion and solvent evaporation process¹⁸². This graphene-based composite material with 14 nm MnFe₂O₄ nanoparticles shows very high T_2 relaxation time with relaxivity value (r_2) of 256.2 (mM Fe)^{–1} s^{–1} and the PEGylated form of the composite is highly biocompatible¹⁸².

Gene delivery

Graphene and graphene composite-based gene delivery system has been developed and proven effective for DNA¹⁸³ or siRNA¹⁸⁴ delivery. Single stranded (ss) RNA or DNA is not stable in cellular delivery due to enzymatic instability. Nanoscale graphene oxide has been used for protecting DNA from cleavage and its effective cellular delivery due to less toxicity of graphene oxide and strong adsorption of DNA on graphene surface¹⁸³. PEGylated reduced graphene oxide (PEG–RGO) nanovector has been used for efficient delivery of ssRNA, where ssRNA itself exhibits poor cellular uptake due to its negative charges and enzyme instability¹⁸⁵. Schneider *et al.*¹⁸⁶ demonstrated the translocation of individual DNA molecules through ultrathin nanopores in graphene. They fabricated nanopores of 22 nm diameter in graphene (using electron beam) and studied the translocation of individual DNA molecule through the nanopore confirmed by the change in the conductance of the nanopore.

Therapeutic applications

Photodynamic therapy (PDT) and photothermal therapy (PTT) are advantageous due to undesired side effects and limited specificity of the commonly used chemotherapy

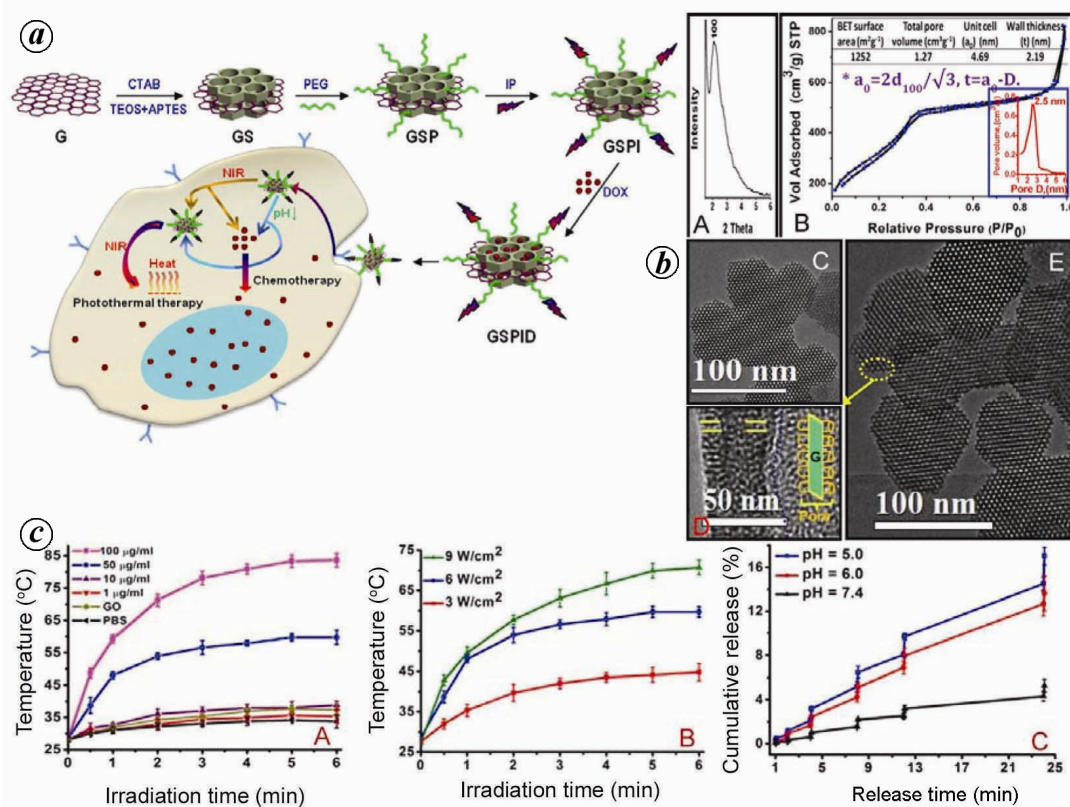


Figure 9. *a*, Schematic of chemo-photothermal targeted therapy of glioma using silica-coated graphene-based multifunctional drug carrier (GSPID). *b*, (A) Small-angle XRD pattern. (B) N₂ adsorption-desorption isotherm for surface area and pore size. (C–E) TEM images of silica-coated graphene. *c*, (A) Photothermal heating profile of IL-13 peptide (IP) modified silica-coated graphene (GSP) solution with varying graphene-silica (GS) composite concentrations at the power intensity of 6 W/cm². (B) Photothermal heating profile of GSP with varying power intensities at constant GS concentration of 50 μg/ml. (C) Cumulative drug release profiles from GSPID at different pH values at the power intensity of 6 W/cm² NIR irradiation. (Figures have been adapted from the Wang *et al.*¹⁹¹ with the permission of ACS Publications, 2013.)

and radiotherapy techniques. In PTT, the therapeutic agent must absorb light and produce heat, which increases the local temperature inside the body and kills the desired tumour cells. Graphene-based materials are good for photothermal agents as they absorb strongly in NIR region. There are few reviews on the therapeutic applications of graphene and graphene oxide^{187,188}. A powerful photothermal agent based on polyethylene glycol (PEG) functionalized graphene oxide (GO-PEG) was studied for *in vivo* cancer treatment. Yang *et al.*¹⁸⁹ have developed PEGylated nano-reduced graphene oxide (average diameter ~27 nm) for ultra-low power photothermal therapy. They have shown that the surface chemistry and size of graphene are important for PTT applications. They observed all the treated mice for 100 days without any death or side effect¹⁸⁹. The same group has developed a multifunctional nanocomposite of PEGylated GO-iron oxide (IONP)-Au, which is even better as a photothermal therapeutic agent than RGO-PEG composite due to enhanced NIR absorbance¹⁹⁰. These GO-IONP-Au-PEG composites can be applied for magnetic resonance (MR) and X-ray dual-mode imaging due to the presence of both

magnetic particles and plasmonic Au nanoparticles. Recently, Wang *et al.*¹⁹¹ combined chemotherapy and photothermal targeted therapy for the design of multifunctional, mesoporous, silica-coated graphene nanosheets as a drug delivery system. Mesoporous silica on graphene increases the surface area, hydrophobicity, dispersibility and functionalities of the system, which exhibits synergic effect of drug loading via π - π interactions and adsorption in the pores¹⁹¹. The schematic mechanism and details of the photo-generated temperature enhancement upon irradiation have been depicted in Figure 9.

In PDT, reactive oxygen species (ROS) generated from photosensitizer upon irradiation are responsible for killing the tumorous cells. Huang *et al.*¹⁹² have reported folic acid-conjugated graphene oxide (GO) loaded with a photosensitizer chlorin e6 (Ce6), due to hydrophobic interactions and π - π stacking. This novel composite is stabilized, which acts as an efficient targeting and photodynamic agent with higher specificity. The photosensitizer Ce6 significantly accumulates in the tumour cells and shows good photodynamic efficiency on MGC803 cells upon irradiation¹⁹².

Table 2. Different biosensing applications of graphene-based hybrid materials

System	Detection method	Analyte	Detection linear range	Detection limit	Reference
CeO ₂ -graphene	Electrogenerated chemiluminescence	Cholesterol	12 μM to 7.2 mM	4.0 μM	200
Graphene-silica-gold NP hybrids	Electrochemical impedance spectroscopy	DNA	10 ⁻¹⁴ to 10 ⁻¹⁰ M	10 fM	201
Perylene derivative/graphene	Electrochemical impedance spectroscopy	<i>Pol</i> gene of HIV-1	1.0 × 10 ⁻¹² to 1.0 × 10 ⁻⁶ M	5.5 × 10 ⁻¹³ M	202
Graphene-CdS	Cyclic voltammetry	Glucose	2.0 to 16 mM	0.7 mM	203
Graphene-AuPd (1 : 1)	Cyclic voltammograms	Glucose	Upper limit up to 3.5 mM	6.9 μM	204
Graphene-polyaniline composite	Cyclic voltammetry and electrochemical impedance spectroscopy	Dopamine	0.007 to 90 nmol/l	0.00198 nmol/l	205
TiO ₂ -graphene	Amperometric response	Glucose	0 to 8 mM	–	206
Porphyrin-functionalized graphene	Electrochemiluminescence	Human telomerase activity	10 to 750 cells/ml	10 HeLa cells/ml	207
Graphene-aptamer-Au nps	Electrochemical impedance spectroscopy and cyclic voltammetry	ATP/Hg ²⁺	ATP: 15 × 10 ⁻⁹ to 4 × 10 ⁻³ M Hg ²⁺ : 0.5–500 nM	15 nm/0.5 nM	208
BaYF ₅ : Yb Er/Tm-graphene oxide	Fluorescence resonance energy transfer	Ochratoxin A/ Fumonisin B1	0.05 to 100 ng ml ⁻¹ 0.1 to 500 ng ml ⁻¹	0.02 ng ml ⁻¹ 0.1 ng ml ⁻¹	209
Graphene-silica-Au hybrids	Differential pulse voltammetry	ATP	0.05 to 56.5 nM	2.3 × 10 ⁻¹¹ M	210
Graphene-Au nps	Square wave voltammetry	L-Histidine	10 pm to 10 mM	0.1 pM	211
Graphene-silica-Au hybrids	Differential pulse voltammetry	D-Vasopressin	5 ng ml ⁻¹ to 56.5 mg ml ⁻¹	5 ng ml ⁻¹	212
Dye-labelled aptamer/graphene oxide	Forster resonance energy transfer	Cancer cells (CCRF-CEM)	2.5 × 10 ¹ to 2.5 × 10 ⁴ cells ml ⁻¹	25 cells ml ⁻¹	213
Graphene-carbon dot@Ag	Electrochemiluminescence	Cancer cells (HeLa cell)	10 to 1 × 10 ⁵ cells ml ⁻¹	10 cells ml ⁻¹	214
Aptamer-graphene oxide	Fluorescence quenching	Pathogen (<i>Salmonella enterica</i> and <i>Staphylococcus aureus</i>)	42.2–675.0 cfu ml ⁻¹ for <i>S. enterica</i> 10 ⁴ to 10 ⁶ cfu ml ⁻¹ for <i>S. aureus</i>	11.0 cfu ml ⁻¹	215
EDTA-modified graphene	Differential pulse voltammogram	Dopamine	0.20–25 μM	0.01 μM	216
rGO-UCNPs (NaYF ₄ : 78 mol% Y ³⁺ , 20 mol% Yb ³⁺ , 2 mol% Er ³⁺)	Electrochemiluminescence	Cyclin A ₂ (prognostic indicator in early-stage cancers)	100 fM to 10 nM	10.5 fM (0.52 pg/ml)	217

Biosensing

Graphene-based materials are important for their ultra-sensitivity and selectivity in sensing of biomolecules like nucleic acids, proteins and cancer cells. Biosensors are based mainly on the optical, electronic, thermal and electrochemical properties of the materials. Graphene-based

materials, having exciting optical, electronic and electrochemical properties and also very high surface area, having diverse functionalities and interactions, are a good choice for sensors and related useful devices as they are eco-friendly, economic, have high sensitivity and are suitable for miniaturization. Various graphene-based hybrid biosensors and their performance have been listed in Table 2.

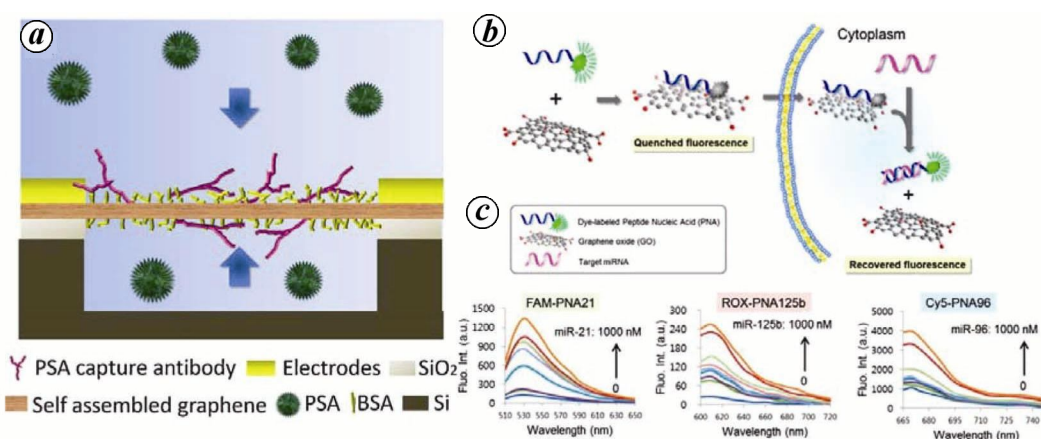


Figure 10. *a*, Schematic of a biosensor based on the change in conductance of graphene modified with PSA capture antibodies for sensing target protein PSA (adapted from Zhang *et al.*¹⁹³ with the permission of Elsevier, 2012). *b*, Scheme of a graphene oxide–peptide nucleic acid built miRNA biosensor based on fluorescence signal on–off. *c*, Three different PNA probes with three different dyes for detection of three different miRNAs; PNA21-FAM, PNA125b-ROX and PNA96-Cy5. (b) and (c) have been adapted from Ryoo *et al.*¹⁹⁴ with the permission of ACS Publications, 2013.

Suspended layer-by-layer self-assembled graphene sensors have been designed by functionalizing graphene with specific anti-PSA antibodies as bioreceptor. This device can detect prostate specific antigen (PSA) down to 0.4 fg/ml (11 aM)¹⁹³ (Figure 10*a*). Ryoo *et al.*¹⁹⁴ have developed a nano graphene oxide–peptide nucleic acid (nGO–PNA) conjugate based miRNA sensor for quantitative detection of targeted miRNA expression levels in living cells with high specificity. The mechanism of the sensing is based on the fluorescence quenching of the dye conjugated to PNA and recovery of the fluorescence upon binding with a target miRNA (Figure 10*b*). This device can sense targeted miRNA with high specificity up to ~1 pM in the living cell¹⁹⁴.

Conclusion and future outlook

Even though graphene chemistry began in the 19th century, it was only after the discovery of graphene by Novoselov in 2004, that significant research started in this area. Due to high mechanical strength and surface area, electronic and thermal properties and its wide range of applications in various fields such as energy conversion, energy storage, transparent electrodes, biological and biomedical, etc. graphene has become one of the most well-studied materials. Among all the synthetic methods gram-scale synthesis of graphene is possible using chemical/sonochemical exfoliation followed by reduction from graphite oxide. These chemical/sonochemical exfoliation and reduction methods are suitable and cost-effective for producing graphene-based composites for catalysis, energy storage, energy conversion and biological applications, whereas for electronic devices CVD is the most suitable method to obtain control over the size, defects and layers of graphene. Elemental metal

(Fe, Zn)-based reductions of graphene oxide are environmentally benign and give better quality of reduced graphene oxide with respect to defects and electronic properties than that of common reduction using hydrazine and sodium borohydride. Significant development in graphene-based composites as catalytic materials, energy storage, energy conversions, drug/gene delivery, therapeutic and biosensors has been thoroughly discussed. Graphene-based composites such as graphene–Fe₃O₄, graphene–SiO₂, graphene–Au and graphene–PEG are extraordinarily effective for biological and medical applications.

Large-scale, cost-effective, green synthesis of graphene sheets with control over size, number of layers, shape and functionalities needs significant effort. Instead of CVD, bottom-up approaches in wet chemical route for the synthesis of good quality graphene from molecules in a large scale have to be explored for future electronics. The electronic properties of graphene synthesized by wet chemical routes have to be improved for large-scale applications. Despite the remarkable applications of graphene-based composites, it has to be functionalized properly for *in vivo* applications.

1. Savage, N., Super carbon. *Nature*, 2012, **483**, S30–S31.
2. Wang, H. *et al.*, Graphene-based materials: fabrication, characterization and application for the decontamination of wastewater and wastegas and hydrogen storage/generation. *Adv. Colloid Interface Sci.*, 2013, **195–196**, 19–40.
3. Castro Neto, A. H., Guinea, F., Peres, N. M. R., Novoselov, K. S. and Geim, A. K. The electronic properties of graphene. *Rev. Mod. Phys.*, 2009, **81**, 109–162.
4. Novoselov, K. S. *et al.*, Electric field effect in atomically thin carbon films. *Science*, 2004, **306**, 666–669.
5. Nair, R. R. *et al.*, Fine structure constant defines visual transparency of graphene. *Science*, 2008, **320**, 1308.
6. Stankovich, S. *et al.*, Graphene-based composite materials. *Nature*, 2006, **442**, 282–286.

7. Li, X., Wang, X., Zhang, L., Lee, S. and Dai, H., Chemically derived, ultrasoft graphene nanoribbon semiconductors. *Science*, 2008, **319**, 1229–1232.
8. Mao, S., Yu, K., Chang, J., Steeber, D. A., Ocola, L. E. and Chen, J., Direct growth of vertically-oriented graphene for field-effect transistor biosensor. *Sci. Rep.*, 2013, **3**, 1696–1702.
9. Li, W., Tan, C., Lowe, M. A., Abruna, H. D. and Ralph, D. C., Electrochemistry of individual monolayer graphene sheets. *ACS Nano*, 2011, **5**, 2264–2270.
10. Ramanathan, T. *et al.*, Functionalized graphene sheets for polymer nanocomposites. *Nature Nanotechnol.*, 2008, **3**, 327–331.
11. Stoller, M. D., Park, S., Zhu, Y., An, J. and Ruoff, R. S., Graphene-based ultracapacitors. *Nano Lett.*, 2008, **8**, 3498–3502.
12. Pumera, M., Graphene in biosensing. *Mater. Today*, 2011, **14**, 308–315.
13. El-Kady, M. F., Strong, V., Dubin, S. and Kaner, R. B., Laser scribing of high-performance and flexible graphene-based electrochemical capacitors. *Science*, 2012, **335**, 1326–1330.
14. Bianco, A., Graphene: safe or toxic? the two faces of the medal. *Angew. Chem., Int. Engl.*, 2013, **52**, 4986–4997.
15. Kotchey, G. P. *et al.*, The enzymatic oxidation of graphene oxide. *ACS Nano*, 2011, **5**, 2098–2108.
16. Jr., W. S. H. and Offeman, R. E., Preparation of graphitic oxide. *J. Am. Chem. Soc.*, 1958, **80**, 1939.
17. Avouris, P., Graphene: electronic and photonic properties and devices. *Nano Lett.*, 2010, **10**, 4285–4294.
18. Huang, X., Zeng, Z., Fan, Z., Liu, J. and Zhang, H., Graphene-based electrodes. *Adv. Mater.*, 2012, **24**, 5979–6004.
19. Bae, S. *et al.*, Roll-to-roll production of 30-inch graphene films for transparent electrodes. *Nature Nanotechnol.*, 2010, **5**, 574–578.
20. Brodie, B. C., Sur le poids atomique du graphite. *Ann. Chim. Phys.*, 1860, **59**, 466.
21. Schaffhaeuti, C., On the combination of carbon with silicon and iron and other metals, forming the different species of cast iron, steel and malleable iron. *Philos. Mag.*, 1840, **16**, 570–590.
22. Novoselov, K. S. *et al.*, Electric field effect in atomically thin carbon films. *Science*, 2004, **306**, 666–669.
23. Rao, C. N. R., Sood, A. K., Subrahmanyam, K. S. and Govindaraj, A., Graphene: the new two-dimensional nanomaterial. *Angew. Chem., Int. Engl.*, 2009, **48**, 7752–7777.
24. Wei, D. and Liu, Y., Controllable synthesis of graphene and its applications. *Adv. Mater.*, 2010, **22**, 3225–3241.
25. Zhu, Y., Murali, S., Cai, W., Li, X., Suk, J. W., Potts, J. R. and Ruoff, R. S., Graphene and graphene oxide: synthesis, properties, and applications. *Adv. Mater.*, 2010, **22**, 3906–3924.
26. Zhu, Y., James, D. K. and Tour, J. M., New routes to graphene, graphene oxide and their related applications. *Adv. Mater.*, 2012, **24**, 4924–4955.
27. Rodríguez-Pérez, L., Herranz, M. Á. and Martín, N., The chemistry of pristine graphene. *Chem. Commun.*, 2013, **49**, 3721–3735.
28. Allen, M. J., Tung, V. C. and Kaner, R. B., Honeycomb carbon: a review of graphene. *Chem. Rev.*, 2010, **110**, 132–145.
29. Georgakilas, V. *et al.*, Functionalization of graphene: covalent and non-covalent approaches, derivatives and applications. *Chem. Rev.*, 2012, **112**, 6156–6214.
30. Chen, D., Feng, H. and Li, J., Graphene oxide: preparation, functionalization and electrochemical applications. *Chem. Rev.*, 2012, **112**, 6027–6053.
31. Mao, H. Y., Laurent, S., Chen, W., Akhavan, O., Imani, M., Ashkarran, A. A. and Mahmoudi, M., Graphene: promises, facts, opportunities and challenges in nanomedicine. *Chem. Rev.*, 2013, **113**, 3407–3424.
32. Xu, M., Liang, T., Shi, M. and Chen, H., Graphene-like two-dimensional materials. *Chem. Rev.*, 2013, **113**, 3766–3798.
33. Dreyer, D. R., Park, S., Bielawski, C. W. and Ruoff, R. S., The chemistry of graphene oxide. *Chem. Soc. Rev.*, 2010, **39**, 228–240.
34. Hass, J., de Heer, W. A. and Conrad, E. H., The growth and morphology of epitaxial multilayer graphene. *J. Phys. Condens. Matter*, 2008, **20**, 323202.
35. Loh, K. P., Bao, Q., Ang, P. K. and Yang, J., The chemistry of graphene. *J. Mater. Chem.*, 2010, **20**, 2277.
36. Sun, Z., James, D. K. and Tour, J. M., Graphene chemistry: synthesis and manipulation. *J. Phys. Chem. Lett.*, 2011, **2**, 2425–2432.
37. Geim, A. K. and Novoselov, K. S., The rise of graphene. *Nature Mater.*, 2007, **6**, 183–191.
38. Park, S. and Ruoff, R. S., Chemical methods for the production of graphenes. *Nature Nanotechnol.*, 2009, **4**, 217–224.
39. Rao, C. N. R. *et al.*, A study of the synthetic methods and properties of graphenes. *Sci. Technol. Adv. Mater.*, 2010, **11**, 054502.
40. Huang, X. *et al.*, Graphene-based materials: synthesis, characterization, properties and applications. *Small*, 2011, **7**, 1876–1902.
41. Luo, B., Liu, S. and Zhi, L., Chemical approaches toward graphene-based nanomaterials and their applications in energy-related areas. *Small*, 2012, **8**, 630–646.
42. Jiang, H., Chemical preparation of graphene-based nanomaterials and their applications in chemical and biological sensors. *Small*, 2011.
43. Shinde, D. B., Debgupta, J., Kushwaha, A., Aslam, M. and Pillai, V. K., Electrochemical unzipping of multi-walled carbon nanotubes for facile synthesis of high-quality graphene nanoribbons. *J. Am. Chem. Soc.*, 2011, **133**, 4168–4171.
44. Geim, A. K., Graphene: status and prospects. *Science*, 2009, **324**, 1530–1534.
45. Lin, Y.-M., Jenkins, K. A., Valdes-Garcia, A., Small, J. P., Farmer, D. B. and Avouris, P., Operation of graphene transistors at gigahertz frequencies. *Nano Lett.*, 2009, **9**, 422–426.
46. Schedin, F., Geim, A. K., Morozov, S. V., Hill, E. W., Blake, P., Katsnelson, M. I. and Novoselov, K. S., Detection of individual gas molecules adsorbed on graphene. *Nature Mater.*, 2007, **6**, 652–655.
47. Stankovich, S. *et al.*, Graphene-based composite materials. *Nature*, 2006, **442**, 282–286.
48. Stankovich, S. *et al.*, Synthesis of graphene-based nanosheets via chemical reduction of exfoliated graphite oxide. *Carbon N. Y.*, 2007, **45**, 1558–1565.
49. He, Q. *et al.*, Centimeter-long and large-scale micropatterns of reduced graphene oxide Films: fabrication and sensing applications. *ACS Nano*, 2010, **4**, 3201–3208.
50. Sudibya, H. G., He, Q., Zhang, H. and Chen, P., Electrical detection of metal ions using field-effect transistors based on micropatterned reduced graphene oxide films. *ACS Nano*, 2011, **5**, 1990–1994.
51. Stankovich, S., Piner, R. D., Chen, X., Wu, N., Nguyen, S. T. and Ruoff, R. S., Stable aqueous dispersions of graphitic nanoplatelets via the reduction of exfoliated graphite oxide in the presence of poly(sodium 4-styrenesulfonate). *J. Mater. Chem.*, 2006, **16**, 155–158.
52. Mcallister, M. J. *et al.*, Single sheet functionalized graphene by oxidation and thermal expansion of graphite. *Chem. Mater.*, 2007, **19**, 4396–4404.
53. Mattevi, C. *et al.*, Evolution of electrical, chemical and structural properties of transparent and conducting chemically derived graphene thin films. *Adv. Funct. Mater.*, 2009, **19**, 2577–2583.
54. Li, D., Müller, M. B., Gilje, S., Kaner, R. B. and Wallace, G. G., Processable aqueous dispersions of graphene nanosheets. *Nature Nanotechnol.*, 2008, **3**, 101–105.

55. Hirata, M., Gotou, T., Horiuchi, S., Fujiwara, M. and Ohba, M., Thin-film particles of graphite oxide. 1: high-yield synthesis and flexibility of the particles. *Carbon N. Y.*, 2004, **42**, 2929–2937.
56. Hirata, M., Gotou, T. and Ohba, M., Thin-film particles of graphite oxide. 2: preliminary studies for internal micro fabrication of single particle and carbonaceous electronic circuits. *Carbon N. Y.*, 2005, **43**, 503–510.
57. Titelman, G. I., Gelman, V., Bron, S., Khalfin, R. L., Cohen, Y. and Bianco-Peled, H., Characteristics and microstructure of aqueous colloidal dispersions of graphite oxide. *Carbon N. Y.*, 2005, **43**, 641–649.
58. Liu, P. and Gong, K., Synthesis of polyaniline-intercalated graphite oxide by an *in situ* oxidative polymerization reaction. *Carbon N. Y.*, 1999, **37**, 701–711.
59. Lomeda, J. R., Doyle, C. D., Kosynkin, D. V., Hwang, W.-F. and Tour, J. M., Diazonium functionalization of surfactant-wrapped chemically converted graphene sheets. *J. Am. Chem. Soc.*, 2008, **130**, 16201–16206.
60. Tung, V. C., Allen, M. J., Yang, Y. and Kaner, R. B., High-throughput solution processing of large-scale graphene. *Nature Nanotechnol.*, 2009, **4**, 25–29.
61. Gómez-Navarro, C., Weitz, R. T., Bittner, A. M., Scolari, M., Mews, A., Burghard, M. and Kern, K., Electronic transport properties of individual chemically reduced graphene oxide sheets. *Nano Lett.*, 2007, **7**, 3499–3503.
62. Becerril, H. A., Mao, J., Liu, Z., Stoltenberg, R. M., Bao, Z. and Chen, Y., Evaluation of solution-processed reduced graphene oxide films as transparent conductors. *ACS Nano*, 2008, **2**, 463–470.
63. Mauro, M., Cipolletti, V., Galimberti, M., Longo, P. and Guerra, G., Chemically reduced graphite oxide with improved shape anisotropy. *J. Phys. Chem. C*, 2012, **116**, 24809–24813.
64. Yang, J., Yan, X., Chen, F., Fan, P. and Zhong, M., Graphite oxide platelets functionalized by poly(ionic liquid) brushes and their chemical reduction. *J. Nanopart. Res.*, 2012, **15**, 1383–1395.
65. Li, Y., Zhao, N., Shi, C., Liu, E. and He, C., Improve the supercapacity performance of MnO₂-decorated graphene by controlling the oxidization extent of graphene. *J. Phys. Chem. C*, 2012, **116**, 25226–25232.
66. Cassagneau, T. and Fendler, J. H., Preparation and layer-by-layer self-assembly of silver nanoparticles capped by graphite oxide nanosheets. *J. Phys. Chem. B*, 1999, **103**, 1789–1793.
67. Gao, W., Alemany, L. B., Ci, L. and Ajayan, P. M., New insights into the structure and reduction of graphite oxide. *Nature Chem.*, 2009, **1**, 403–408.
68. Shin, H.-J. *et al.*, Efficient reduction of graphite oxide by sodium borohydride and its effect on electrical conductance. *Adv. Funct. Mater.*, 2009, **19**, 1987–1992.
69. Muszynski, R., Seger, B. and Kamat, P. V., Decorating graphene sheets with gold nanoparticles. *J. Phys. Chem. C*, 2008, **112**, 5263–5266.
70. He, Y. and Cui, H., Synthesis of dendritic platinum nanoparticles/lucigenin/reduced graphene oxide hybrid with chemiluminescence activity. *Chem. Eur. J.*, 2012, **18**, 4823–4826.
71. Chua, C. K. and Pumera, M., Reduction of graphene oxide with substituted borohydrides. *J. Mater. Chem. A*, 2013, **1**, 1892–1898.
72. Wang, G., Yang, J., Park, J., Gou, X., Wang, B., Liu, H. and Yao, J., Facile synthesis and characterization of graphene nanosheets. *J. Phys. Chem. C*, 2008, **112**, 8192–8195.
73. Bao, Q., Zhang, D. and Qi, P., Synthesis and characterization of silver nanoparticle and graphene oxide nanosheet composites as a bactericidal agent for water disinfection. *J. Colloid Interface Sci.*, 2011, **360**, 463–470.
74. Gurunathan, S., Han, J. W., Dayem, A. A., Eppakayala, V. and Kim, J.-H., Oxidative stress-mediated antibacterial activity of graphene oxide and reduced graphene oxide in *Pseudomonas aeruginosa*. *Int. J. Nanomedicine*, 2012, **7**, 5901–5914.
75. Gurunathan, S., Han, J. W., Eppakayala, V. and Kim, J.-H., Green synthesis of graphene and its cytotoxic effects in human breast cancer cells. *Int. J. Nanomed.*, 2013, **8**, 1015–1027.
76. Gurunathan, S., Han, J. W. and Kim, J.-H., Green chemistry approach for the synthesis of biocompatible graphene. *Int. J. Nanomed.*, 2013, **8**, 2719–2732.
77. Fan, X., Peng, W., Li, Y., Li, X., Wang, S., Zhang, G. and Zhang, F., Deoxygenation of exfoliated graphite oxide under alkaline conditions: a green route to graphene preparation. *Adv. Mater.*, 2008, **20**, 4490–4493.
78. Guo, H., Wang, X., Qian, Q., Wang, F. and Xia, X., A green approach to the synthesis of graphene nanosheets. *ACS Nano*, 2009, **3**, 2653–2659.
79. Liu, S., Wang, J., Zeng, J., Ou, J., Li, Z., Liu, X. and Yang, S., ‘Green’ electrochemical synthesis of Pt/graphene sheet nanocomposite film and its electrocatalytic property. *J. Power Sources*, 2010, **195**, 4628–4633.
80. Zhu, C., Guo, S., Fang, Y. and Dong, S., Reducing sugar: new functional molecules for the green synthesis of graphene nanosheets. *ACS Nano*, 2010, **4**, 2429–2437.
81. He, H. and Gao, C., Supraparamagnetic, conductive and processable multifunctional graphene nanosheets coated with high-density Fe₃O₄ nanoparticles. *ACS Appl. Mater. Interfaces*, 2010, **2**, 3201–3210.
82. Liu, X.-W., Yao, Z.-J., Wang, Y.-F. and Wei, X.-W., Graphene oxide sheet-Prussian blue nanocomposites: green synthesis and their extraordinary electrochemical properties. *Colloids Surf. B*, 2010, **81**, 508–512.
83. Fan, Z.-J. *et al.*, Facile synthesis of graphene nanosheets via Fe reduction of exfoliated graphite oxide. *ACS Nano*, 2011, **5**, 191–198.
84. Dey, R. S., Hajra, S., Sahu, R. K., Raj, R. C. and Panigrahi, M. K., A rapid room temperature chemical route for the synthesis of graphene: metal-mediated reduction of graphene oxide. *Chem. Commun.*, 2012, **48**, 1787–1789.
85. Wang, Y., Shi, Z. and Yin, J., Facile synthesis of soluble graphene via a green reduction of graphene oxide in tea solution and its biocomposites. *ACS Appl. Mater. Interfaces*, 2011, **3**, 1127–1133.
86. Zhang, J., Yang, H., Shen, G., Cheng, P., Zhang, J. and Guo, S., Reduction of graphene oxide via l-ascorbic acid. *Chem. Commun.*, 2010, **46**, 1112–1114.
87. Mhamane, D. *et al.*, From graphite oxide to highly water dispersible functionalized graphene by single step plant extract-induced deoxygenation. *Green Chem.*, 2011, **13**, 1990–1996.
88. Thakur, S. and Karak, N., Green reduction of graphene oxide by aqueous phytoextracts. *Carbon N. Y.*, 2012, **50**, 5331–5339.
89. Budi Nursanto, E., Nugroho, A., Hong, S.-A., Kim, S. J., Yoon Chung, K. and Kim, J., Facile synthesis of reduced graphene oxide in supercritical alcohols and its lithium storage capacity. *Green Chem.*, 2011, **13**, 2714–2718.
90. Liu, K., Zhang, J.-J., Cheng, F.-F., Zheng, T.-T., Wang, C. and Zhu, J.-J., Green and facile synthesis of highly biocompatible graphene nanosheets and its application for cellular imaging and drug delivery. *J. Mater. Chem.*, 2011, **21**, 12034–12040.
91. Singh, V. V. *et al.*, Greener electrochemical synthesis of high quality graphene nanosheets directly from pencil and its SPR sensing application. *Adv. Funct. Mater.*, 2012, **22**, 2352–2362.
92. Liu, J., Fu, S., Yuan, B., Li, Y. and Deng, Z., Toward a universal ‘adhesive nanosheet’ for the assembly of multiple nanoparticles based on a protein-induced reduction/decoration of graphene oxide. *J. Am. Chem. Soc.*, 2010, **132**, 7279–7281.

93. Liu, Y., Li, Y., Zhong, M., Yang, Y. and Wang, M., A green and ultrafast approach to the synthesis of scalable graphene nanosheets with Zn powder for electrochemical energy storage. *J. Mater. Chem.*, 2011, **21**, 15449–15455.
94. Zhang, Y. *et al.*, One-pot green synthesis of Ag nanoparticles-graphene nanocomposites and their applications in SERS, H₂O₂, and glucose sensing. *RSC Adv.*, 2012, **2**, 538–545.
95. Zhang, Y. *et al.*, Biomolecule-assisted, environmentally friendly, one-pot synthesis of CuS/reduced graphene oxide nanocomposites with enhanced photocatalytic performance. *Langmuir*, 2012, **28**, 12893–12900.
96. Shah, M. S. A. S., Park, A. R., Zhang, K., Park, J. H. and Yoo, P. J., Green synthesis of biphasic TiO₂-reduced graphene oxide nanocomposites with highly enhanced photocatalytic activity. *ACS Appl. Mater. Interfaces*, 2012, **4**, 3893–3901.
97. Gupta, S. S., Sreepasad, T. S., Maliyekkal, S. M., Das, S. K. and Pradeep, T., Graphene from sugar and its application in water purification. *ACS Appl. Mater. Interfaces*, 2012, **4**, 4156–4163.
98. Chen, X., Su, B., Wu, G., Yang, C. J., Zhuang, Z., Wang, X. and Chen, X., Platinum nanoflowers supported on graphene oxide nanosheets: their green synthesis, growth mechanism and advanced electrocatalytic properties for methanol oxidation. *J. Mater. Chem.*, 2012, **22**, 11284–11289.
99. Sui, Z., Meng, Q., Zhang, X., Mab, R. and Cao, B., Green synthesis of carbon nanotube-graphene hybrid aerogels and their use as versatile agents for water purification. *J. Mater. Chem.*, 2012, **22**, 8767–8771.
100. Zhang, Y., Wang, X., Zeng, L., Song, S. and Liu, D., Green and controlled synthesis of Cu₂O-graphene hierarchical nanohybrids as high-performance anode materials for lithium-ion batteries via an ultrasound assisted approach. *Dalton Trans.*, 2012, **41**, 4316–4319.
101. Wang, X., Li, X., Liu, D., Song, S. and Zhang, H., Green synthesis of Pt/CeO₂/graphene hybrid nanomaterials with remarkably enhanced electrocatalytic properties. *Chem. Commun.*, 2012, **48**, 2885–2887.
102. Wang, X., Huang, P., Feng, L., He, M., Guo, S., Shen, G. and Cui, D., Green controllable synthesis of silver nanomaterials on graphene oxide sheets via spontaneous reduction. *RSC Adv.*, 2012, **2**, 3816–3822.
103. Wang, Y., Zhang, P., Fang Liu, C., Zhan, L., Fang Li, Y. and Huang, C. Z., Green and easy synthesis of biocompatible graphene for use as an anticoagulant. *RSC Adv.*, 2012, **2**, 2322–2328.
104. Aravind, S. S. J., Eswaraiah, V. and Ramaprabhu, S., Facile and simultaneous production of metal/metal oxide dispersed graphene nano composites by solar exfoliation. *J. Mater. Chem.*, 2011, **21**, 17094–17097.
105. Wallace, P. R., The band theory of graphite. *Phys. Rev.*, 1947, **71**, 622–634.
106. Sreepasad, T. S. and Berry, V., How do the electrical properties of graphene change with its functionalization? *Small*, 2013, **9**, 341–350.
107. Son, D. I. *et al.*, Emissive ZnO-graphene quantum dots for white-light-emitting diodes. *Nature Nanotechnol.*, 2012, **7**, 465–471.
108. Chen, C., Cai, W., Long, M., Zhou, B., Wu, Y., Wu, D. and Feng, Y., Synthesis of visible-light responsive graphene oxide/TiO₂ composites with p/n heterojunction. *ACS Nano*, 2010, **4**, 6425–6432.
109. Zhang, Y. *et al.*, Direct observation of a widely tunable bandgap in bilayer graphene. *Nature*, 2009, **459**, 820–823.
110. Samarakoon, D. K. and Wang, X.-Q., Tunable band gap in hydrogenated bilayer graphene. *ACS Nano*, 2010, **4**, 4126–4130.
111. Lee, D. H. *et al.*, Engineering electronic properties of graphene by coupling with Si-rich, two-dimensional islands. *ACS Nano*, 2013, **7**, 301–307.
112. Wei, D., Liu, Y., Wang, Y., Zhang, H., Huang, L. and Yu, G., Synthesis of N-doped graphene by chemical vapour deposition and its electrical properties. *Nano Lett.*, 2009, **9**, 1752–1758.
113. Panchakarla, L. S., Subrahmanyam, K. S., Saha, S. K., Govindaraj, A., Krishnamurthy, H. R., Waghmare, U. V. and Rao, C. N. R., Synthesis, structure and properties of boron- and nitrogen-doped graphene. *Adv. Mater.*, 2009, **21**, 4726–4730.
114. Kim, J. *et al.*, Electrical control of optical plasmon resonance with graphene. *Nano Lett.*, 2012, **12**, 5598–5602.
115. Chen, J. *et al.*, Optical nano-imaging of gate-tunable graphene plasmons. *Nature*, 2012, **487**, 77–81.
116. Shen, J., Zhu, Y., Yang, X. and Li, C., Graphene quantum dots: emergent nanolights for bioimaging, sensors, catalysis and photovoltaic devices. *Chem. Commun.*, 2012, **48**, 3686–3699.
117. Zhu, S. *et al.*, Strongly green-photoluminescent graphene quantum dots for bioimaging applications. *Chem. Commun.*, 2011, **47**, 6858–6860.
118. Shinde, D. B. and Pillai, V. K., Electrochemical preparation of luminescent graphene quantum dots from multiwalled carbon nanotubes. *Chem. Eur. J.*, 2012, **18**, 12522–12528.
119. Shinde, D. B. and Pillai, V. K., Electrochemical resolution of multiple redox events for graphene quantum dots. *Angew. Chem. Int. Ed. Engl.*, 2013, **52**, 2482–2485.
120. Wang, H.-X., Wang, Q., Zhou, K.-G. and Zhang, H.-L., Graphene in light: design, synthesis and applications of photo-active graphene and graphene-like materials. *Small*, 2013, **9**, 1266–1283.
121. Tu, W., Zhou, Y. and Zou, Z., Versatile graphene-promoting photocatalytic performance of semiconductors: basic principles, synthesis, solar energy conversion and environmental applications. *Adv. Funct. Mater.*, 2013, **23**, 4996–5008.
122. Zhang, H., Lv, X., Li, Y., Wang, Y. and Li, J., P25-graphene composite as a high performance photocatalyst. *ACS Nano*, 2010, **4**, 380–386.
123. Chen, F.-J., Cao, Y.-L. and Jia, D.-Z., A room-temperature solid-state route for the synthesis of graphene oxide-metal sulfide composites with excellent photocatalytic activity. *CrystEngComm*, 2013, **15**, 4747–4754.
124. Tu, X., Luo, S., Chen, G. and Li, J., One-pot synthesis, characterization, and enhanced photocatalytic activity of a BioBr-graphene composite. *Chem., Eur. J.*, 2012, **18**, 14359–14366.
125. Ramesha, G. K., Kumara, A. V., Muralidhara, H. B. and Sampath, S., Graphene and graphene oxide as effective adsorbents toward anionic and cationic dyes. *J. Colloid Interface Sci.*, 2011, **361**, 270–277.
126. Das, D., Shivhare, A., Saha, S. and Ganguli, A. K., Room temperature synthesis of mesoporous TiO₂ nanostructures with high photocatalytic efficiency. *Mater. Res. Bull.*, 2012, **11**, 3780–3785.
127. Tian, C., Zhang, Q., Wu, A., Jiang, M., Liang, Z., Jiang, B. and Fu, H., Cost-effective large-scale synthesis of ZnO photocatalyst with excellent performance for dye photodegradation. *Chem. Commun.*, 2012, **48**, 2858–2860.
128. Lee, J. S., You, K. H. and Park, C. B., Highly photoactive, low bandgap TiO₂ nanoparticles wrapped by graphene. *Adv. Mater.*, 2012, **24**, 1084–1088.
129. Huang, Q. *et al.*, Enhanced photocatalytic activity of chemically bonded TiO₂/graphene composites based on the effective interfacial charge transfer through the C-Ti bond. *ACS Catal.*, 2013, **3**, 1477–1485.
130. Zhu, M., Chen, P. and Liu, M., Ag/AgBr/graphene oxide nanocomposite synthesized via oil/water and water/oil micro-emulsions: a comparison of sunlight energized plasmonic photocatalytic activity. *Langmuir*, 2012, **28**, 3385–3390.
131. Zhu, M., Chen, P. and Liu, M., High-performance visible-light-driven plasmonic photocatalysts Ag/AgCl with controlled size

- and shape using graphene oxide as capping agent and catalyst promoter. *Langmuir*, 2013, **29**, 9259–9268.
132. Li, Q., Guo, B., Yu, J., Ran, J., Zhang, B., Yan, H. and Gong, J. R., Highly efficient visible-light-driven photocatalytic hydrogen production of CdS-cluster-decorated graphene nanosheets. *J. Am. Chem. Soc.*, 2011, **133**, 10878–10884.
 133. Xiang, Q., Yu, J. and Jaroniec, M., Synergetic effect of MoS₂ and graphene as cocatalysts for enhanced photocatalytic H₂ production activity of TiO₂ nanoparticles. *J. Am. Chem. Soc.*, 2012, **134**, 6575–6578.
 134. Zhang, X., Wang, B., Sunarso, J., Liu, S. and Zhi, L., Graphene nanostructures toward clean energy technology applications. *Wiley Interdiscip. Rev. Energy Environ.*, 2012, **1**, 317–336.
 135. Li, N., Liu, G., Zhen, C., Li, F., Zhang, L. and Cheng, H.-M., Battery performance and photocatalytic activity of mesoporous anatase TiO₂ nanospheres/graphene composites by template-free self-assembly. *Adv. Funct. Mater.*, 2011, **21**, 1717–1722.
 136. Yang, S. *et al.*, Bottom-up approach toward single-crystalline VO₂-graphene ribbons as cathodes for ultrafast lithium storage. *Nano Lett.*, 2013, **13**, 1596–1601.
 137. Nethravathi, C., Viswanath, B., Michael, J. and Rajamath, M., Hydrothermal synthesis of a monoclinic VO₂ nanotube-graphene hybrid for use as cathode material in lithium ion batteries. *Carbon N. Y.*, 2012, **50**, 4839–4846.
 138. Wang, X. *et al.*, N-doped graphene-SnO₂ sandwich paper for high-performance lithium-ion batteries. *Adv. Funct. Mater.*, 2012, **22**, 2682–2690.
 139. Zhong, C., Wang, J., Chen, Z. and Liu, H., SnO₂-graphene composite synthesized via an ultrafast and environmentally friendly microwave autoclave method and its use as a superior anode for lithium-ion batteries. *J. Phys. Chem. C*, 2011, **115**, 25115–25120.
 140. Zhou, X., Wan, L. and Guo, Y., Binding SnO₂ nanocrystals in nitrogen-doped graphene sheets as anode materials for lithium-ion batteries. *Adv. Mater.*, 2013, **25**, 2152–2157.
 141. Wang, D. *et al.*, Layer by layer assembly of sandwiched graphene/SnO₂ nanorod/carbon nanostructures with ultrahigh lithium ion storage properties. *Energy Environ. Sci.*, 2013, **6**, 2900–2906.
 142. Li, Y., Lv, X., Lu, J. and Li, J., Preparation of SnO₂-nanocrystal/graphene-nanosheets composites and their lithium storage ability. *J. Phys. Chem. C*, 2010, **114**, 21770–21774.
 143. Wang, D. *et al.*, Ternary self-assembly of ordered metal oxide-graphene nanocomposites for electrochemical energy storage. *ACS Nano*, 2010, **4**, 1587–1595.
 144. Vinayan, B. P. and Ramaprabhu, S., Facile synthesis of SnO₂ nanoparticles dispersed nitrogen doped graphene anode material for ultrahigh capacity lithium ion battery applications. *J. Mater. Chem. A*, 2013, **1**, 3865–3871.
 145. Shiva, K., Rajendra, H. B., Subrahmanyam, K. S., Bhattacharyya, A. J. and Rao, C. N. R., Improved lithium cyclability and storage in mesoporous SnO₂ electronically wired with very low concentrations (<1%) of reduced graphene oxide. *Chem., A Eur. J.*, 2012, **18**, 4489–4494.
 146. Wu, Z. *et al.*, Graphene anchored with Co₃O₄ nanoparticles as anode of lithium ion capacity and cyclic performance. *ACS Nano*, 2010, **4**, 3187–3194.
 147. Zhu, J. *et al.*, Facile preparation of ordered porous graphene-metal oxide@C binder-free electrodes with high Li storage performance. *Small*, 2013, **9**, 3390–3397.
 148. Jiang, Y., Yuan, T., Sun, W. and Yan, M., Electrostatic spray deposition of porous SnO₂/graphene anode films and their enhanced Lithium-storage properties. *ACS Appl. Mater. Interfaces*, 2012, **4**, 6216–6220.
 149. Niu, C., Sichel, E. K., Hoch, R., Moy, D. and Tennent, H., High power electrochemical capacitors based on carbon nanotube electrodes. *Appl. Phys. Lett.*, 1997, **70**, 1480–1482.
 150. Stoller, M. D., Park, S., Zhu, Y., An, J. and Ruoff, R. S., Graphene-based ultracapacitors. *Nano Lett.*, 2008, **8**, 3498–3502.
 151. Zhu, Y. *et al.*, Carbon-based supercapacitors produced by activation of graphene. *Science*, 2011, **332**, 1537–1541.
 152. Liu, C., Yu, Z., Neff, D., Zhamu, A. and Jang, B. Z., Graphene-based supercapacitor with an ultrahigh energy density. *Nano Lett.*, 2010, **10**, 4863–4868.
 153. Wu, Q., Xu, Y., Yao, Z., Liu, A. and Shi, G., Supercapacitors based on flexible graphene/polyaniline nanofiber composite films. *ACS Nano*, 2010, **4**, 1963–1970.
 154. Mishra, A. K. and Ramaprabhu, S., Functionalized graphene-based nanocomposites for supercapacitor application. *J. Phys. Chem. C*, 2011, **115**, 14006–14013.
 155. Huang, Y., Liang, J. and Chen, Y., An overview of the applications of graphene-based materials in supercapacitors. *Small*, 2012, **8**, 1805–1834.
 156. Li, H., Zou, L., Pan, L. and Sun, Z., Novel graphene-like electrodes for capacitive deionization. *Environ. Sci. Technol.*, 2010, **44**, 8692–8697.
 157. Gabelich, C. J., Tran, T. D. and Suffet, I. H. M., Electrosorption of inorganic salts from aqueous solution using carbon aerogels. *Environ. Sci. Technol.*, 2002, **36**, 3010–3019.
 158. Rana-Madaria, P., Nagarajan, M., Rajagopal, C. and Garg, B. S., Removal of chromium from aqueous solutions by treatment with carbon aerogel electrodes using response surface methodology. *Ind. Eng. Chem. Res.*, 2005, **44**, 6549–6559.
 159. Huang, Z.-H., Wang, M., Wang, L. and Kang, F., Relation between the charge efficiency of activated carbon fiber and its desalination performance. *Langmuir*, 2012, **28**, 5079–5084.
 160. Oda, H. and Nakagawa, Y., Removal of ionic substances from dilute solution using activated carbon electrodes. *Carbon N. Y.*, 2003, **41**, 1037–1047.
 161. Li, L., Zou, L., Song, H. and Morris, G., Ordered mesoporous carbons synthesized by a modified sol-gel process for electrosorptive removal of sodium chloride. *Carbon N. Y.*, 2009, **47**, 775–781.
 162. Peng, Z. *et al.*, Comparative electroadsorption study of mesoporous carbon electrodes with various pore structures. *J. Phys. Chem. C*, 2011, **115**, 17068–17076.
 163. Wang, L. *et al.*, Capacitive deionization of NaCl solutions using carbon nanotube sponge electrodes. *J. Mater. Chem.*, 2011, **21**, 18295.
 164. Peng, H., Meng, L., Lu, Q., Dong, S., Fei, Z. and Dyson, P. J., Fabrication of reduced graphene oxide hybrid materials that exhibit strong fluorescence. *J. Mater. Chem.*, 2012, **22**, 14868.
 165. Sreepasad, T. S., Maliyekkal, S. M., Lisha, K. P. and Pradeep, T., Reduced graphene oxide-metal/metal oxide composites: facile synthesis and application in water purification. *J. Hazard. Mater.*, 2011, **186**, 921–931.
 166. Wimalasiri, Y. and Zou, L., Carbon nanotube/graphene composite for enhanced capacitive deionization performance. *Carbon N. Y.*, 2013, **59**, 464–471.
 167. Wang, Z., Dou, B., Zheng, L., Zhang, G., Liu, Z. and Hao, Z., Effective desalination by capacitive deionization with functional graphene nanocomposite as novel electrode material. *Desalination*, 2012, **299**, 96–102.
 168. Wen, X., Zhang, D., Yan, T., Zhang, J. and Shi, L., Three-dimensional graphene-based hierarchically porous carbon composites prepared by a dual-template strategy for capacitive deionization. *J. Mater. Chem. A*, 2013, **1**, 12334.
 169. Sint, K., Wang, B. and Kra, P., Selective ion passage through functionalized graphene nanopores. *J. Am. Chem. Soc.*, 2008, **130**, 16448–16449.
 170. Zhao, J., Ren, W. and Cheng, H.-M., Graphene sponge for efficient and repeatable adsorption and desorption of water contaminations. *J. Mater. Chem.*, 2012, **22**, 20197.

171. Chandra, V., Park, J., Chun, Y., Lee, J. W., Hwang, I. and Kim, K. S., Water-dispersible magnetite-reduced graphene oxide composites for arsenic removal. *ACS Nano*, 2010, **4**, 3979–3986.
172. Chandra, V. and Kim, K. S., Highly selective adsorption of Hg^{2+} by a polypyrrole-reduced graphene oxide composite. *Chem. Commun.*, 2011, **47**, 3942–3944.
173. Zhu, J. *et al.*, One-pot synthesis of magnetic graphene nanocomposites decorated with core@double-shell nanoparticles for fast chromium removal. *Environ. Sci. Technol.*, 2012, **46**, 977–985.
174. Wang, Y., Liang, S., Chen, B., Guo, F., Yu, S. and Tang, Y., Synergistic removal of Pb(II), Cd(II) and humic acid by Fe_3O_4 @mesoporous silica-graphene oxide composites. *PLoS One*, 2013, **8**, e65634.
175. Fan, L., Luo, C., Sun, M., Li, X. and Qiu, H., Highly selective adsorption of lead ions by water-dispersible magnetic chitosan/graphene oxide composites. *Colloids Surf. B. Biointerfaces*, 2013, **103**, 523–529.
176. Alghomhi, W. M., Bandaru, N. M., Yu, Y., Shapter, J. G. and Ellis, A. V., Alginate–graphene oxide hybrid gel beads: an efficient copper adsorbent material. *J. Colloid Interface Sci.*, 2013, **397**, 32–38.
177. Deliyanni, E. A., Peleka, E. N. and Matis, K. A., Removal of zinc ion from water by sorption onto iron-based nano-adsorbent. *J. Hazard. Mater.*, 2007, **141**, 176–184.
178. Zhang, K., Dwivedi, V., Chi, C. and Wu, J., Graphene oxide/ferric hydroxide composites for efficient arsenate removal from drinking water. *J. Hazard. Mater.*, 2010, **182**, 162–168.
179. Fan, X., Jiao, G., Zhao, W., Jina, P. and Li, X., Magnetic Fe_3O_4 -graphene composites as targeted drug nanocarriers for pH-activated release. *Nanoscale*, 2013, **5**, 1143–1152.
180. Yang, X., Zhang, X., Ma, Y., Huang, Y., Wang, Y. and Chen, Y., Superparamagnetic graphene oxide– Fe_3O_4 nanoparticles hybrid for controlled targeted drug carriers. *J. Mater. Chem.*, 2009, **19**, 2710–2714.
181. Ma, X. *et al.*, A functionalized graphene oxide–iron oxide nanocomposite for magnetically targeted drug delivery, photothermal therapy and magnetic resonance imaging. *Nano Res.*, 2012, **5**, 199–212.
182. Peng, E., Choo, E. S. G., Chandrasekharan, P., Yang, C.-T., Ding, J., Chuang, K.-H. and Xue, J. M., Synthesis of manganese ferrite/graphene oxide nanocomposites for biomedical applications. *Small*, 2012, **8**, 3620–3630.
183. Lu, C.-H., Zhu, C.-L., Li, J., Liu, J.-J., Chen, X. and Yang, H.-H., Using graphene to protect DNA from cleavage during cellular delivery. *Chem. Commun.*, 2010, **46**, 3116–3118.
184. Yang, X., Niu, G., Cao, X., Wen, Y., Xiang, R., Duan, H. and Chen, Y., The preparation of functionalized graphene oxide for targeted intracellular delivery of siRNA. *J. Mater. Chem.*, 2012, **22**, 6649–6654.
185. Zhang, L. *et al.*, PEGylated reduced graphene oxide as a superior ssRNA delivery system. *J. Mater. Chem. B*, 2013, **1**, 749–755.
186. Schneider, G. F., Kowalczyk, S. W., Calado, V. E., Pandraud, G., Zandbergen, H. W., Vandersypen, L. M. K. and Dekker, C., DNA translocation through graphene nanopores. *Nano Lett.*, 2010, **10**, 3163–3167.
187. Feng, L., Wu, L. and Qu, X., New horizons for diagnostics and therapeutic applications of graphene and graphene oxide. *Adv. Mater.*, 2013, **25**, 168–186.
188. Yang, K., Feng, L., Shi, X. and Liu, Z., Nano-graphene in biomedicine: theranostic applications. *Chem. Soc. Rev.*, 2013, **42**, 530–547.
189. Yang, K., Wan, J., Zhang, S., Tian, B., Zhang, Y. and Liu, Z., The influence of surface chemistry and size of nanoscale graphene oxide on photothermal therapy of cancer using ultra-low laser power. *Biomaterials*, 2012, **33**, 2206–2214.
190. Shi, X., Gong, H., Li, Y., Wang, C., Cheng, L. and Liu, Z., Graphene-based magnetic plasmonic nanocomposite for dual bioimaging and photothermal therapy. *Biomaterials*, 2013, **34**, 4786–4793.
191. Wang, Y., Wang, K., Zhao, J., Liu, X., Bu, J., Yan, X. and Huang, R., Multifunctional mesoporous silica-coated graphene nanosheet used for chemo-photothermal synergistic targeted therapy of glioma. *J. Am. Chem. Soc.*, 2013, **135**, 4799–4804.
192. Huang, P. *et al.*, Folic acid-conjugated graphene oxide loaded with photosensitizers for targeting photodynamic therapy. *Theranostics*, 2011, **1**, 240–250.
193. Zhang, B., Li, Q. and Cui, T., Ultra-sensitive suspended graphene nanocomposite cancer sensors with strong suppression of electrical noise. *Biosens. Bioelectron.*, 2012, **31**, 105–109.
194. Ryoo, S. *et al.*, Quantitative and multiplexed microRNA sensing in living cells based on peptide nucleic acid and nano graphene oxide (PANGO). *ACS Nano*, 2013, **7**, 5882–5891.
195. Zhang, X., Chen, Y. L., Liu, R.-S. and Tsai, D. P., Plasmonic photocatalysis. *Rep. Prog. Phys.*, 2013, **76**, 046401–046441.
196. Perera, S. D., Mariano, R. G., Vu, K., Nour, N., Seitz, O., Chabal, Y. and Balkus Jr, K. J., Hydrothermal synthesis of graphene-TiO₂ nanotube composites with enhanced photocatalytic activity. *ACS Catal.*, 2012, **2**, 949–956.
197. Yang, N., Liu, Y., Wen, H., Tang, Z., Zhao, H., Li, Y. and Wang, D., Photocatalytic properties of graphdiyne and graphene modified TiO₂: from theory to experiment. *ACS Nano*, 2013, **7**, 1504–1512.
198. Xiang, Q., Yu, J. and Jaroniec, M., Preparation and enhanced visible-light photocatalytic H₂ production activity of graphene/C₃N₄ composites. *J. Phys. Chem. C*, 2011, **115**, 7355–7363.
199. Bai, X., Wang, L., Zong, R., Lv, Y., Sun, Y. and Zhu, Y., Performance enhancement of ZnO photocatalyst via synergic effect of surface oxygen defect and graphene hybridization. *Langmuir*, 2013, **29**, 3097–3105.
200. Zhang, M., Yuan, R., Chai, Y., Wang, C. and Wu, X., Cerium Oxide-graphene as the matrix for cholesterol sensor. *Anal. Biochem.*, 2013, **436**, 69–74.
201. Du, Y., Guo, S., Dong, S. and Wang, E., An integrated sensing system for detection of DNA using new parallel-motif DNA triplex system and graphene-mesoporous silica-gold nanoparticle hybrids. *Biomaterials*, 2011, **32**, 8584–8592.
202. Hu, Y., Wang, K., Zhang, Q., Li, F., Wu, T. and Niu, L., Decorated graphene sheets for label-free dna impedance biosensing. *Biomaterials*, 2012, **33**, 1097–1106.
203. Wang, K., Liu, Q., Guan, Q.-M., Wu, J., Li, H.-N. and Yan, J.-J., Enhanced direct electrochemistry of glucose oxidase and biosensing for glucose via synergy effect of graphene and CdS nanocrystals. *Biosens. Bioelectron.*, 2011, **26**, 2252–2257.
204. Yang, J., Deng, S., Lei, J., Ju, H. and Gunasekaran, S., Electrochemical synthesis of reduced graphene sheet–AuPd alloy nanoparticle composites for enzymatic biosensing. *Biosens. Bioelectron.*, 2011, **29**, 159–166.
205. Liu, S., Xing, X., Yu, J., Lian, W., Li, J., Cui, M. and Huang, J., A novel label-free electrochemical aptasensor based on graphene-polyaniline composite film for dopamine determination. *Biosens. Bioelectron.*, 2012, **36**, 186–191.
206. Jang, H. D., Kim, S. K., Chang, H., Roh, K.-M., Choi, J.-W. and Huang, J., A glucose biosensor based on TiO₂-graphene composite. *Biosens. Bioelectron.*, 2012, **38**, 184–188.
207. Wu, L., Wang, J., Feng, L., Ren, J., Wei, W. and Qu, X., Label-free ultrasensitive detection of human telomerase activity using porphyrin-functionalized graphene and electrochemiluminescence technique. *Adv. Mater.*, 2012, **24**, 2447–2452.
208. Wang, L., Xu, M., Han, L., Zhou, M., Zhu, C. and Dong, S., Graphene enhanced electron transfer at aptamer modified electrode and its application in biosensing. *Anal. Chem.*, 2012, **84**, 7301–7307.

209. Wu, S., Duan, N., Ma, X., Xia, Y., Wang, H., Wang, Z. and Zhang, Q., Multiplexed fluorescence resonance energy transfer aptasensor between upconversion nanoparticles and graphene oxide for the simultaneous determination of mycotoxins. *Anal. Chem.*, 2012, **84**, 6263–6270.
210. Guo, S., Du, Y., Yang, X., Dong, S. and Wang, E., Solid-state label-free integrated aptasensor based on graphene-mesoporous silica? Gold nanoparticle hybrids and silver microspheres. *Anal. Chem.*, 2011, **83**, 8035–8040.
211. Liang, J., Chen, Z., Guo, L. and Li, L., Electrochemical sensing of L-histidine based on structure-switching DNAzymes and gold nanoparticle–graphene nanosheet composites. *Chem. Commun.*, 2011, **47**, 5476–5478.
212. Du, Y., Guo, S., Qin, H., Dong, S. and Wang, E., Target-induced conjunction of split aptamer as new chiral selector for oligopeptide on graphene-mesoporous silica-gold nanoparticle hybrids modified sensing platform. *Chem. Commun.*, 2012, **48**, 799–801.
213. Cao, L. *et al.*, Visual and high-throughput detection of cancer cells using a graphene oxide-based FRET aptasensing microfluidic chip. *Lab Chip*, 2012, **12**, 4864–4869.
214. Wu, L., Wang, J., Ren, J., Li, W. and Qu, X., Highly sensitive electrochemiluminescent cytosensing using carbon nanodot@Ag hybrid material and graphene for dual signal amplification. *Chem. Commun.*, 2013, **49**, 5675–5677.
215. Zuo, P., Li, X., Dominguez, D. C. and Ye, B.-C., A PDMS/paper/glass hybrid microfluidic biochip integrated with aptamer-functionalized graphene oxide nano-biosensors for one-step multiplexed pathogen detection. *Lab Chip*, 2013, **13**, 3921–3928.
216. Hou, S., Kasner, M. L., Su, S., Patel, K. and Cuellari, R., Highly sensitive and selective dopamine biosensor fabricated with silanized graphene. *J. Phys. Chem. C*, 2010, **114**, 14915–14921.
217. Wu, L., Wang, J., Yin, M., Ren, J., Miyoshi, D., Sugimoto, N. and Qu, X., Reduced graphene oxide upconversion nanoparticle hybrid for electrochemiluminescent sensing of a prognostic indicator in early-stage cancer. *Small*, 2013, **10**, 330–336.

ACKNOWLEDGEMENTS. A.K.G. thanks CSIR and DST, New Delhi for financial support. K.O. thanks UGC, New Delhi for fellowship.